Search for the production of an excited bottom quark decaying to tW in proton-proton collisions at $\sqrt{s} = 8\,\text{TeV}$

The CMS collaboration

E-mail: cms-publication-committee-chair@cern.ch

ABSTRACT: A search is presented for a singly produced excited bottom quark (b^*) decaying to a top quark and a W boson in the all-hadronic, lepton+jets, and dilepton final states in proton-proton collisions at $\sqrt{s} = 8\,\text{TeV}$ recorded by the CMS experiment at the CERN LHC. Data corresponding to an integrated luminosity of $19.7\,\text{fb}^{-1}$ are used. No significant excess of events is observed with respect to standard model expectations. We set limits at 95% confidence on the product of the b^* quark production cross section and its branching fraction to tW. The cross section limits are interpreted for scenarios including left-handed, right-handed, and vector-like couplings of the b^* quark and are presented in the two-dimensional coupling plane based on the production and decay coupling constants. The masses of the left-handed, right-handed, and vector-like b^* quark states are excluded at 95% confidence below 1390, 1430, and 1530 GeV, respectively, for benchmark couplings. This analysis gives the most stringent limits on the mass of the b^* quark to date.

Contents

1 Introduction

Following the discovery of a Higgs boson [1–3], the standard model (SM) may be complete. However, there are phenomena such as baryon asymmetry, neutrino mass, and dark matter, questions of naturalness, and hierarchy problems for which the SM offers no explanation. Various theories with new physics beyond the SM exist that address these problems, including a variety of models that predict the existence of excited quarks, such as Randall-Sundrum models [4, 5] and models with a heavy gluon partner [6–8]. Searches for excited quarks have been performed at the CERN LHC [9–11] and elsewhere [12]. These searches focus on the strong and electroweak interactions of the excited quark with the SM up- or down-type quarks. This paper reports on a search by the CMS Collaboration, using the tW decay mode, for an excited third-generation bottom quark (b*), which preferentially couples to the third-generation SM quarks. A previous search in the same channel by the ATLAS Collaboration resulted in a lower limit on the b* quark mass of about 1 TeV [11]. A search for a b* quark has also been performed in the gb decay mode by CMS [10] resulting
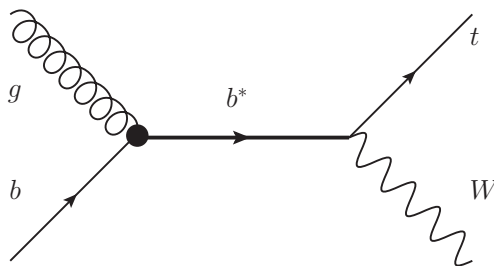
Figure 1. Leading-order Feynman diagram contributing to gb → b* → tW.

in an exclusion region between 1.2 and 1.6 TeV, assuming a branching fraction of 100% for b* decaying to gb.

At the LHC, a b* quark can be produced in a gluon and a bottom quark interaction as shown in figure 1. This interaction is described by the effective Lagrangian:

$$\mathcal{L} = \frac{g_s}{2\,\Lambda} G_{\mu\nu}\, \overline{\mathrm{b}}\, \sigma^{\mu\nu} \left(\kappa_L^{\mathrm{b}} P_L + \kappa_R^{\mathrm{b}} P_R \right) \mathrm{b}^* + \text{Hermitian conjugate (h.c.)}, \tag{1.1}$$

where g_s is the strong coupling, $G_{\mu\nu}$ is the gauge field tensor of the gluon, and Λ [13] is the scale of compositeness, which is chosen to be the mass of the b* quark. The quantities P_L and P_R are the chiral projection operators and κ_L^{b} and κ_R^{b} are the corresponding relative coupling strengths. The branching fractions of b* quark decays are reported in ref. [14]. Possible b* quark decay modes include gb, bZ, bH, and tW. The branching fraction of the b* → tW process increases as a function of b* quark mass and becomes the largest for $m_{\mathrm{b}^*} > 400\,\mathrm{GeV}$, reaching a plateau at almost 40% of the total b* quark decay width.

The decay of interest in this analysis proceeds through the weak interaction as is described by the Lagrangian:

$$\mathcal{L} = \frac{g_2}{\sqrt{2}} \mathrm{W}_\mu^+\, \overline{\mathrm{t}}\, \gamma^\mu \left(g_L P_L + g_R P_R \right) \mathrm{b}^* + \text{h.c.}, \tag{1.2}$$

where g_2 is the weak coupling, and g_L and g_R are the relative coupling strengths of the W boson to the left- and right-handed b* quark, respectively.

This analysis searches for a singly produced b* decaying to a top quark and a W boson. Since there are both left- and right-handed operators in the production and decay interaction Lagrangians, the b* quark could have generic couplings. We consider the benchmark cases of a purely left-handed b* (b$_L^*$) quark with $g_L = 1$, $\kappa_L^{\mathrm{b}} = 1$, $g_R = 0$, $\kappa_R^{\mathrm{b}} = 0$, a purely right-handed b* (b$_R^*$) quark with $g_L = 0$, $\kappa_L^{\mathrm{b}} = 0$, $g_R = 1$, $\kappa_R^{\mathrm{b}} = 1$, and a vector-like b* quark with $g_L = 1$, $\kappa_L^{\mathrm{b}} = 1$, $g_R = 1$, $\kappa_R^{\mathrm{b}} = 1$.

The analysis is performed in three different channels distinguished by the number of leptons (electrons and muons) appearing in the b* → tW → bWW decay. The all-hadronic channel has two jets: one from a boosted top quark and the other from the boosted W boson. As the Lorentz boosts of the top quark and W boson increase, the angular distance between their direct decay products decreases, leading to only two resolvable jets. The lepton+jets channel has one lepton, one b jet, two light-flavor (u-, d-, s-quark) or gluon

jets, and significant transverse momentum (p_T) imbalance. The dilepton channel has two leptons, at least one jet, and significant p_T imbalance.

2   The CMS detector

The central feature of the CMS apparatus is a superconducting solenoid of 6 m internal diameter, providing a magnetic field of 3.8 T. Within the solenoid volume are a silicon pixel and strip tracker, a lead tungstate crystal electromagnetic calorimeter (ECAL), and a brass and scintillator hadron calorimeter, each composed of a barrel and two endcap sections. Forward calorimeters extend the pseudorapidity coverage provided by the barrel and endcap detectors. Muons are measured in gas-ionization detectors embedded in the steel flux-return yoke outside the solenoid. A detailed description of the CMS detector, together with a definition of the coordinate system used and the relevant kinematic variables, can be found in ref. [15].

3   Signal and background simulations

The simulation of b* quark production and decay is performed with MAD-GRAPH 5.1.5.12 [16] based on the Lagrangian in the b* quark model [14], and uses the CTEQ6L1 parton distribution functions (PDF) set [17]. The renormalization and factorization scales are set to the b* quark mass. The b* quark is forced to decay to tW, with the top quark subsequently decaying into bW. The simulated samples are produced for b* quark masses ranging from 800 to 2000 GeV, in steps of 100 GeV. Left-handed and right-handed b* quark samples are generated. The vector-like b* quark samples are the sum of the right- and left-handed samples. The values for the b* quark production cross section times b*tW branching fraction in proton-proton collisions at a center-of-mass energy of 8 TeV are listed in table 1.

Several simulated background samples are used. The samples for t-channel, tW-channel, and s-channel production of single top quarks, and the $t\bar{t}$ sample are generated using the POWHEG 1.0 event generator [18–20] with the CT10 PDF set [21]. A next-to-next-to-leading-order (NNLO) cross section of 245.8 pb is used for the $t\bar{t}$ sample [22]. The total prediction is normalized to the next-to-next-to-leading-log values of 87.1, 22.2, and 5.55 pb for the t-, tW-, and s-channels, respectively [23].

The Drell-Yan sample (denoted as Z+jets in the following) with the invariant mass of two leptons being greater than 50 GeV, and the W inclusive sample (W+jets) are generated using MADGRAPH with the CTEQ6L1 PDF set. The NNLO cross sections of 3500 pb and 36700 pb are used for the Z+jets and W+jets normalization, respectively [24].

The diboson (WW, WZ, and ZZ) background samples are generated inclusively using PYTHIA 6.426 [25] with the CTEQ6L1 PDF set and normalized to a NNLO cross section of 57.1, 32.3, and 8.26 pb, respectively, calculated from MCFM 6.6 [26].

All of the samples are then interfaced to PYTHIA for parton showering and hadronization, based on the Z2* tune [27]. The generated samples are then passed to the CMS detector simulation based on GEANT4 [28], with alignment and calibration determined

b* quark mass [GeV]	$\sigma_{\mathrm{gb}\to\mathrm{b}^*\to\mathrm{tW}}$ [pb]	b* quark mass [GeV]	$\sigma_{\mathrm{gb}\to\mathrm{b}^*\to\mathrm{tW}}$ [pb]
800	2.98 ± 0.39	1500	0.040 ± 0.006
900	1.45 ± 0.20	1600	0.024 ± 0.004
1000	0.74 ± 0.10	1700	0.014 ± 0.002
1100	0.39 ± 0.06	1800	0.009 ± 0.001
1200	0.21 ± 0.03	1900	0.005 ± 0.001
1300	0.12 ± 0.02	2000	0.003 ± 0.001
1400	0.07 ± 0.01		

Table 1. Estimates of the total cross section for $\mathrm{gb} \to \mathrm{b}^*$ at a center of mass energy of 8 TeV times the branching fraction for $\mathrm{b}^* \to \mathrm{tW}$ for b* quark masses from 800 to 2000 GeV. The values are identical for left-handed and right-handed quark hypotheses. The uncertainties are determined by varying the factorization (μ_F) and renormalization (μ_R) scales simultaneously by a factor of 0.5 or 2 of their nominal value. The estimated cross section of a b* quark with vector-like coupling is twice as large at each mass point as the value shown.

from data or dedicated calibration samples. The average number of pileup interactions (additional inelastic proton-proton collisions within the same bunch crossing) is observed to be approximately 20 for the data recorded in 2012. Proton-proton collisions are added to simulated signal and background events so that the distribution of reconstructed primary vertices agrees with what is observed in data.

4 Trigger, event quality, and object selection

At least one reconstructed primary vertex that is associated with at least four reconstructed tracks [29] is required to be present in the event.

Events that are due to beam halo, poor calibration, and malfunctioning detector electronics are rejected. The particle-flow (PF) algorithm [30] is used for both data and simulated events to reconstruct physics objects such as electrons, muons, and charged and neutral hadrons.

Electron candidates are reconstructed within the range of pseudorapidity $|\eta| < 2.5$ using the energy clusters in the ECAL [31]. The clusters are associated with charged-particle tracks reconstructed in the tracking detector. The absolute value of the electron candidate transverse impact parameter should be smaller than 0.02 cm. Identified electrons from photon conversions are vetoed. The relative isolation requires $I_{\mathrm{rel}} < 0.1$, where I_{rel} is the ratio of the sum of the p_{T} of other particles around the electron candidate to the p_{T} of the electron candidate. The p_{T} summation is over the charged hadrons, photons, and neutral hadrons, in a cone size of $\Delta R = \sqrt{(\Delta\eta)^2 + (\Delta\phi)^2} < 0.3$, where ϕ is the azimuthal angle in radians. The estimated contribution from pileup is removed from the sum on an event-by-event basis [32]. Electron candidates with clusters in the transition region between barrel and endcap ($1.4442 < |\eta| < 1.5660$) are removed since the electron reconstruction is

not optimal in this region. The p_{T} of the electron candidate is required to be larger than 30 GeV in the dilepton channel and 130 GeV for the lepton+jets channel.

Muon candidates are reconstructed within $|\eta| < 2.4$ by combining the information from the muon detectors and the inner tracking detectors [33]. For the muon selection used in the lepton+jets channel, a requirement of $|\eta| < 2.1$ is imposed, to match the coverage of the single muon trigger. The candidate's trajectory fit has to satisfy $\chi^2/n < 10$ (where n is the number of degrees of freedom in the fit), have at least one hit in the muon detectors, and have more than five hits in the silicon tracker, of which at least one should be in the pixel detector. The absolute value of the muon candidate transverse impact parameter should be smaller than 0.02 cm. In order to suppress the small background due to cosmic ray muons, the absolute value of the muon candidate longitudinal impact parameter must be less than 0.5 cm. Isolated muons are selected by the requirement $I_{\mathrm{rel}} < 0.12$ in a cone size of $\Delta R < 0.4$ around the muon candidate. The p_{T} of the muon candidate has the same threshold as the electron candidate.

The events are divided into all-hadronic, lepton+jets, and dilepton channels based on the number of leptons (0, 1, or 2 leptons). To suppress possible overlap between lepton+jets and dilepton channels, events with additional electrons (muons) with $p_{\mathrm{T}} > 20$ GeV and $I_{\mathrm{rel}} < 0.15$ (0.2) are rejected.

For the lepton+jets and dilepton analyses, jets are reconstructed by clustering the PF candidates using the anti-k_{T} algorithm [34] implemented by FastJet 3.0.4 [35] with a distance parameter of 0.5. Charged PF particles that are inconsistent with the primary vertex with the highest value of $\sum p_{\mathrm{T}}^2$ are removed from the clustering. This requirement significantly suppresses contamination from charged particles associated with pileup vertices. The neutral component from pileup is removed by applying an estimated residual energy correction based on the jet area [36].

Jets from b quark decays (b jets) are identified with the combined secondary vertex (CSV) b tagging algorithm [37]. This is based on the presence of a displaced secondary vertex in a jet, reconstructed from charged tracks, combined with other quantities comprising track impact parameters, charged hadron kinematic variables, track multiplicity, etc. The tight CSV selection criteria (CSVT) with a misidentification probability of 0.1% for light-flavor jets with an efficiency around 55% for b jets is used.

The negative vector sum of the p_{T} of all the PF candidates ($\vec{E}_{\mathrm{T}}^{\mathrm{miss}}$) is calculated for each event. The magnitude of $\vec{E}_{\mathrm{T}}^{\mathrm{miss}}$ ($E_{\mathrm{T}}^{\mathrm{miss}}$) [30] is used in the lepton+jets and dilepton analysis.

The all-hadronic channel uses a trigger that requires the scalar sum of the transverse momenta of all jet candidates in the event (H_{T}) to be at least 750 GeV. The lepton+jets channel uses a single-electron trigger with a p_{T} threshold of 27 GeV and single-muon trigger with a p_{T} threshold of 24 GeV. The dilepton channel uses the dilepton (ee, eμ, and $\mu\mu$) triggers, with leading and sub-leading lepton p_{T} thresholds of 17 and 8 GeV, respectively.

In the all-hadronic channel, the selected W bosons and top quarks are sufficiently energetic for their decay products to have a large Lorentz boost and are reconstructed as single jets. Such jets are identified within $|\eta| < 2.4$ using the jet decomposition into subjets, followed by application of criteria based on the kinematic properties of subjets. The Cambridge-Aachen (CA) algorithm [38] with distance parameter of 0.8 is used to

cluster jets that are considered for the W boson and top quark selections, instead of the anti-k_T algorithm that is used in the lepton+jets and dilepton analyses.

The identification of a boosted W boson (W tagging) attempts to identify the two daughter quarks of the W boson by using the N-subjettiness [39] variable:

$$\tau_\mathrm{N} = \frac{1}{d_0} \sum_i p_{\mathrm{T}i} \, \min\{\Delta R_{1i}, \Delta R_{2i}, \ldots, \Delta R_{Ni}\}, \tag{4.1}$$

where ΔR_{ji} is the angular separation between the axis of the subjet candidate j and the axis of the constituent particle i, and d_0 is a normalization factor. The variable τ_N is a p_T-weighted angular distance from a jet constituent to the nearest subjet axis, and is close to zero if a given jet is consistent with having N or fewer subjets. The τ_2/τ_1 ratio is used to discriminate between the signal W-tagged jets with two subjets and jets from light quarks and gluons with a single hard subjet ($\tau_2/\tau_1 < 0.5$). In addition, jet pruning [40] is used to remove soft and wide-angle radiation, which significantly reduces the measured mass of QCD multijet events, while leaving the measured mass of W-tagged jets close to the nominal W boson mass. The mass of the pruned jet is required to be consistent with the W boson mass ($70 < m_\mathrm{jet} < 100\,\mathrm{GeV}$). The difference in W tagging efficiency between data and simulation is corrected by a simulation-to-data scale factor derived from the W+jets and dijet control samples [41].

Boosted top quark identification (t tagging) discriminates signal from background events by using the three-prong substructure of a merged t jet. We use the CMS t tagging algorithm [42], which reclusters the jet until it finds one to four subjets that are consistent with daughters of the top quark decay [43]. We require at least three subjets and determine the lowest mass m_min of the pairwise combinations of the three highest-p_T subjets. This m_min is required to be compatible with the mass of the W boson ($m_\mathrm{min} > 50\,\mathrm{GeV}$). Finally, the mass of the CA jet from the t tagging algorithm is required to be consistent with the top quark mass ($140 < m_\mathrm{jet} < 250\,\mathrm{GeV}$).

The t tagging selection in this analysis also uses N-subjettiness discrimination. In this case the variable of interest is τ_3/τ_2, since t jets are expected to have three subjets ($\tau_3/\tau_2 < 0.55$). Exactly one of the three subjets originating from the top quark decay should be a b jet, which we identify by requiring the largest subjet CSV discriminator value to satisfy the medium selection criteria. This requirement has a misidentification probability of 0.1% for light-flavor jets and an efficiency of around 65% for b jets [44].

This t tagging algorithm was studied in lepton+jets data and simulated samples enriched in top quarks with high Lorentz boost. We use a simulation-to-data scale factor for t tagging derived from these studies to correct the Monte Carlo (MC) samples in the all-hadronic channel [45].

5 Event selection and background estimation

We search for the presence of a b* quark decaying to tW by looking for deviations from the expected background in the distributions of kinematic variables for the all-hadronic, lepton+jets, and dilepton channels. The event selections and background estimations of these three channels are presented below.

5.1 All-hadronic channel

The all-hadronic channel is characterized by a top quark and a W boson, both of which decay hadronically. After the trigger selection, exactly two CA jets with p_T of at least $425\,\mathrm{GeV}$ are required to be present in the event. One high-p_T jet is required to be W-tagged, while the other is required to be t-tagged. The main backgrounds for this channel are $t\bar{t}$ and multijet events, which are estimated using control regions in data. The small background contribution from single top quark production is estimated from simulation.

The multijet contribution is estimated by applying the top quark mistagging (t mistagging) rate on events before t tagging is applied. We measure the t mistagging rate using a control region where the contribution of signal events is suppressed. For this control region we select a W-tagged jet in the region of $30 < m_\mathrm{jet} < 70\,\mathrm{GeV}$ or $m_\mathrm{jet} > 100\,\mathrm{GeV}$. After applying this selection we take the ratio of the number of jets that are t-tagged to the number of all top quark candidate jets to define the t mistagging rate. Here we use the t tagging algorithm described in section 4 but exclude the top quark candidate mass requirement that is applied to the pre-tagged top quark candidate jets. The $t\bar{t}$ contamination is determined from simulation and is accounted for when extracting the t mistagging rate. The $t\bar{t}$ fraction in this region is about 25% of the post-tag sample (numerator) and 1% of the pre-tag sample (denominator). To extract a multijet background estimate, we weight the events that pass the pre-t-tagged selection by the t mistagging rate. The parameterization of the t mistagging rate is done as a function of the candidate jet p_T and $|\eta|$, in order to account for kinematic correlations inherent in t tagging. The mass distribution of the top quark candidate in the multijet background estimate is corrected on a bin-by-bin basis by a weight extracted from simulation, to correct for differences in the top quark candidate mass spectrum before and after t tagging. This correction is such that it only changes the shape of the distribution and has no effect on the overall normalization. The correction factor depends on the mass of the top quark candidate and ranges from 0.45 at low mass to 2.25 at high mass. The corresponding change in shape of the m_tW spectrum is taken into account in the systematic uncertainties, and makes a contribution that is much smaller than the total systematic uncertainty, shown in figure 2 as the hatched band.

The contribution from $t\bar{t}$ production is estimated by using a control region defined by requiring one of the jets to pass inverted W tagging requirements: $m_\mathrm{jet} > 130\,\mathrm{GeV}$ and $\tau_2/\tau_1 > 0.5$. This selection has an enhanced $t\bar{t}$ fraction. We compare the multijet and simulation-based $t\bar{t}$ background estimates to the selection in data, then perform a fit to the invariant mass of the top quark candidate jet. The template-based fit constrains the multijet background template to move within its uncertainties, whereas the normalization on $t\bar{t}$ is unconstrained. This study suggests that, in addition to the scale factors that are applied, the $t\bar{t}$ contribution needs to be further scaled by 0.79 ± 0.17. The uncertainty in this normalization is obtained from the fitting procedure.

The invariant mass of the top quark and W boson candidate jets, m_tW, for the selected events in the signal region is shown in figure 2 and is used for limit setting. The expected number of events is 359 ± 57, and the observed number of events is 318 (table 2).
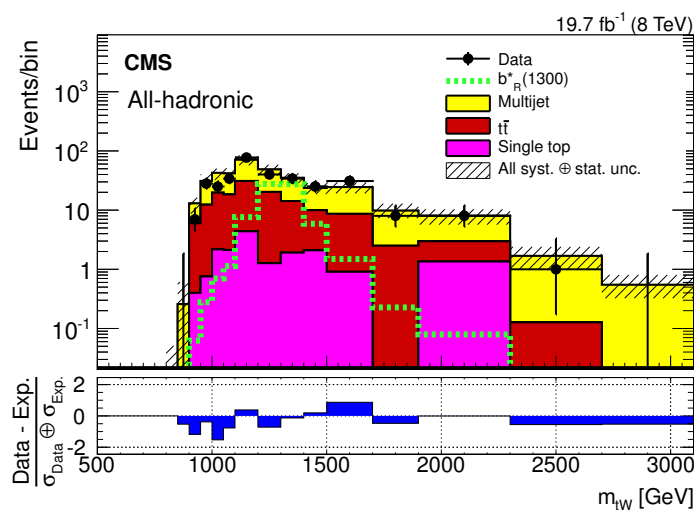
Figure 2. The invariant mass of the tW system in the all-hadronic channel after the full selection of data, the estimated background, and the simulated signal with a b* mass of 1300 GeV. The combined statistical and systematic uncertainties are indicated by the hatched band. The bottom plot shows the pull ((data-background)/$\sigma_{\text{Data}} \oplus \sigma_{\text{Exp.}}$) between the data and the background estimate distributions. The quantities σ_{Data} and $\sigma_{\text{Exp.}}$ refer to the statistical uncertainty in data, and the systematic uncertainty in the background respectively.

Sample		Yield $\pm$ stat. $\pm$ syst.
b_L^*	800 GeV	$26.0 \pm 1.9 \pm 7.4$
b_L^*	1300 GeV	$57.8 \pm 0.6 \pm 4.0$
b_L^*	1800 GeV	$4.1 \pm 0.0 \pm 0.2$
b_R^*	800 GeV	$33.4 \pm 2.2 \pm 9.1$
b_R^*	1300 GeV	$72.5 \pm 0.6 \pm 4.8$
b_R^*	1800 GeV	$5.4 \pm 0.0 \pm 0.3$
$t\bar{t}$		$129 \pm\ \ 3\ \pm 42$
Single top		$19.0 \pm 2.9 \pm 6.5$
Multijet		$211 \pm\ \ 0\ \pm 38$
SM expected		$359 \pm\ \ 4\ \pm 57$
Data		318

Table 2. Event yields in the all-hadronic channel after the final selection, normalized to an integrated luminosity of 19.7 fb^{-1}. Both statistical and systematic uncertainties are shown. The systematic uncertainties are described in section 6.
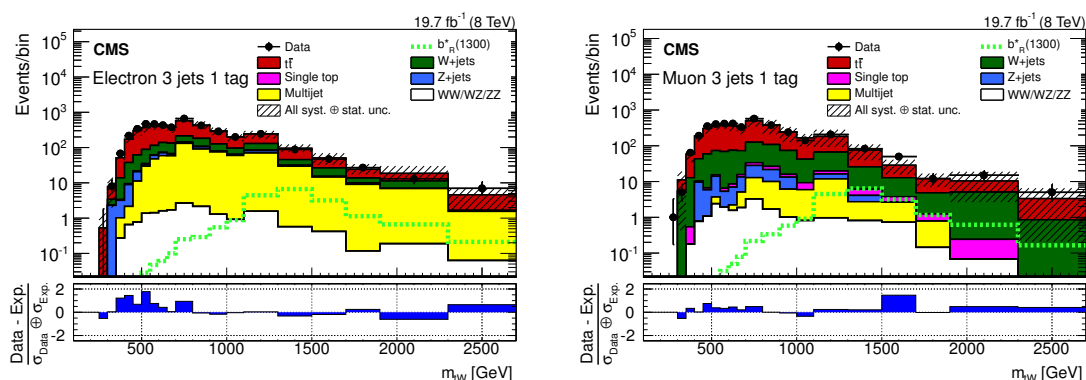
5.2 Lepton+jets channel

The lepton+jets channel is characterized by the presence of exactly one isolated electron or muon and a b jet, as well as at least two light-flavor jets. The signal region is defined to have exactly three jets with $p_T > 40\,\mathrm{GeV}$ and $|\eta| < 2.4$, together with exactly one electron with $p_T > 130\,\mathrm{GeV}$ and $|\eta| < 2.4$, or exactly one muon with $p_T > 130\,\mathrm{GeV}$ and $|\eta| < 2.1$. Of these three jets, there must be exactly one jet that satisfies the CSVT b tagging selection. The contributions of the b^* quark signal, $t\bar{t}$, single top quark, Z+jets, and diboson processes are taken from simulation. The multijet and W+jets background contributions are estimated from data.

The multijet background is estimated by performing a fit to the E_T^{miss} distribution for the electron channel, and a fit to the transverse mass distribution of the leptonically decaying W boson in the muon channel. The choice of the variables used to estimate the background depends on the accuracy with which they are modeled, the choice is different for the electron and muon channels because different subdetectors are involved. A multijet control sample is selected to model the multijet background distributions by reversing the lepton isolation selection criteria to $I_{\mathrm{rel}} > 0.3$; multijet events comprise >99% of this sample. The other backgrounds are modeled using simulated events. The multijet background from the control sample is normalized to the fitted yield to model the multijet background distribution in the signal region. The possibility of a small contamination from a signal is taken into account in fitting the scale factors to backgrounds involving W bosons decaying leptonically.

The W+jets background is estimated by performing a template fit to the distribution of the reconstructed invariant mass of the leptonically decaying W boson and a b jet, $m_{b\ell\nu}$. The fit is performed separately for the electron and muon channels. The p_x and p_y of the neutrino from the W boson decay are set equal to the x and y components of the $\vec{E}_T^{\mathrm{miss}}$. The p_z component is estimated by constraining the reconstructed mass of the W boson to be 80.4 GeV [12], resulting in two solutions. If both solutions are real, the one with the lowest $|p_z|$ is selected. If there is no real solution, p_x and p_y are varied until there is a single solution that minimizes the distance between the neutrino momentum and the missing momentum in the transverse plane. For the fit to the $m_{b\ell\nu}$ distribution, the multijet background template is fixed to the result of the multijet background estimated from data, with the shape taken from the multijet-enriched control region. The SM $t\bar{t}$, single top quark, Z+jets, and diboson templates are taken from the simulation with a common normalization scale factor of 1.09 ± 0.10 obtained from the fit. The W+jets template is taken from the simulation, and normalized to the fitted yield. The possibility of a small contamination from a signal is taken into account in the scale factors applied to backgrounds with a top quark signature.

The expected b^* quark signal and background events and observed data events are listed in table 3 for the electron and muon channels separately.

We search for the b^* signal as an excess above the predicted backgrounds in the distribution of the invariant mass m_{tW} of the lepton, three jets, and $\vec{E}_T^{\mathrm{miss}}$. In this calculation, the neutrino p_x and p_y components are obtained from $\vec{E}_T^{\mathrm{miss}}$, and p_z is set to zero since it cannot be measured by the detector and could have multiple solutions from the analytical second order W mass constraint. The distribution of m_{tW} is shown in figure 3. The widths of the bins are chosen to be comparable to the resolution in the reconstructed m_{tW}.

Sample		Yield $\pm$ stat. $\pm$ syst. Electron channel	Yield $\pm$ stat. $\pm$ syst. Muon channel
b_L^*	800 GeV	$300 \pm\ \ 6\ \pm 50$	$311 \pm\ \ 6\ \pm 51$
b_L^*	1300 GeV	$11.9 \pm 0.2 \pm 3.3$	$12.7 \pm 0.2 \pm 3.5$
b_L^*	1800 GeV	$0.8 \pm 0.0 \pm 0.3$	$0.7 \pm 0.0 \pm 0.3$
b_R^*	800 GeV	$383 \pm\ \ 6\ \pm 63$	$396 \pm\ \ 7\ \pm 66$
b_R^*	1300 GeV	$18.5 \pm 0.2 \pm 5.0$	$18.2 \pm 0.2 \pm 4.9$
b_R^*	1800 GeV	$1.0 \pm 0.0 \pm 0.4$	$1.0 \pm 0.0 \pm 0.4$
$t\bar{t}$		$2581 \pm 23\ \pm 370$	$2736 \pm 23\ \pm 400$
Single top		$364 \pm\ \ 4\ \pm 78$	$387 \pm\ \ 4\ \pm 84$
WW/WZ/ZZ		$17.9 \pm 1.2 \pm 2.7$	$19.4 \pm 1.4 \pm 3.4$
W+jets		$671 \pm 100 \pm 230$	$639 \pm 87\ \pm 150$
Z+jets		$92 \pm\ \ 15 \pm 33$	$80 \pm 13\ \pm 33$
Multijet		$678 \pm 100 \pm 150$	$48\ ^{+\ 78}_{-\ 48}\ \pm 23$
SM expected		$4404 \pm 150 \pm 470$	$3909 \pm 120 \pm 440$
Data		4368	3887

Table 3. Event yields in the lepton+jets channel after the final selection, normalized to an integrated luminosity of $19.7\,\text{fb}^{-1}$. Both statistical and systematic uncertainties are included. The systematic uncertainties are described in section 6.

Figure 3. The invariant mass, m_{tW}, in data compared to the SM background estimation for the electron (left) and muon (right) channels. The combined statistical and systematic uncertainties are indicated by the hatched band. The bottom plots show the pull ((data-background)$/\sigma_{\text{Data}} \oplus \sigma_{\text{Exp.}}$) between the data and the background estimate distributions. The quantities σ_{Data} and $\sigma_{\text{Exp.}}$ refer to the statistical uncertainty in data, and the systematic uncertainty in the background, respectively.

Sample		Yield ± stat. ± syst. ee channel	Yield ± stat. ± syst. eμ channel	Yield ± stat. ± syst. $\mu\mu$ channel
b$_L^*$	800 GeV	$158\pm\ 2\ \pm 32$	$347\pm\ 3\ \pm 72$	$192\pm\ 3\ \pm 39$
b$_L^*$	1300 GeV	$6.4\pm0.1\pm 1.5$	$14.3\pm0.1\pm 3.3$	$7.7\pm0.1\pm 1.7$
b$_L^*$	1800 GeV	$0.4\pm0.0\pm 0.1$	$0.8\pm0.0\pm 0.2$	$0.5\pm0.0\pm 0.1$
b$_R^*$	800 GeV	$203\pm\ 2\ \pm 42$	$452\pm\ 4\ \pm 94$	$243\pm\ 3\ \pm 50$
b$_R^*$	1300 GeV	$7.4\pm0.1\pm 1.7$	$16.5\pm0.1\pm 3.7$	$8.9\pm0.1\pm 2.0$
b$_R^*$	1800 GeV	$0.4\pm0.0\pm 0.1$	$0.9\pm0.0\pm 0.2$	$0.5\pm0.0\pm 0.1$
t$\bar{\text{t}}$		$3157\pm24\pm 530$	$7226\pm40\pm 1220$	$3939\pm29\pm 660$
Single top		$323\pm12\pm 83$	$775\pm19\pm 210$	$414\pm14\pm 110$
WW/WZ/ZZ		$323\pm\ 5\ \pm 110$	$700\pm\ 2\ \pm 240$	$399\pm10\pm 130$
W+jets		$38\pm12\pm 3.2$	$45\pm15\pm 1.4$	$1\pm0.4\pm 0.0$
Z+jets		$553\pm24\pm 130$	$31.6\pm5.0\pm 5.4$	$734\pm29\pm 170$
SM expected		$4396\pm38\pm 558$	$8777\pm47\pm 1257$	$5487\pm45\pm 699$
Data		4583	7873	4988

Table 4. Event yields for the dilepton channel after the final selection, normalized to an integrated luminosity of $19.7\,\text{fb}^{-1}$. Both statistical and systematic uncertainties are included. The systematic uncertainties are described in section 6.

5.3 Dilepton channel

The dilepton channel is characterized by two isolated, oppositely charged electrons or muons and at least one jet. The signal region is defined to have at least one jet with $p_\text{T} > 30\,\text{GeV}$ and $|\eta| < 2.5$, together with at least two leptons having $p_\text{T} > 30\,\text{GeV}$ and $|\eta| < 2.5$ (2.4) for electrons (muons). A minimum distance requirement of 0.3 between the two leptons in ΔR removes photons radiated from muons in W+jets events, which can mimic extra electrons. Most of the diboson background is removed by requiring that the invariant mass of the two leptons is greater than 120 GeV. In addition to the basic selections, events are required to have $E_\text{T}^\text{miss} > 40\,\text{GeV}$. This requirement reduces top quark background by 30%, W+jets background by 50%, diboson events by 60%, and removes over 95% of Z+jets events, while keeping 90% of the signal events. The dominant backgrounds for this channel are t$\bar{\text{t}}$, single top quark, W+jets, Z+jets, and diboson, and are predicted by simulation.

A study is conducted to check the W+jets and multijet backgrounds using same-sign events; the multijet background is found to be negligible, and the W+jets estimate agrees with the MC simulation prediction within the statistical uncertainties. Control regions, defined by reversing the E_T^miss cut or by adding a b tagging requirement, are compared with data to confirm that the dominant background sources are simulated correctly.

We search for the b* quark signal events using the distribution of the scalar sum S_T of the p_T of the two leading leptons, the jet with the highest p_T, and E_T^miss. The distribution of this variable is shown in figure 4. The results of the full selection are listed in table 4.

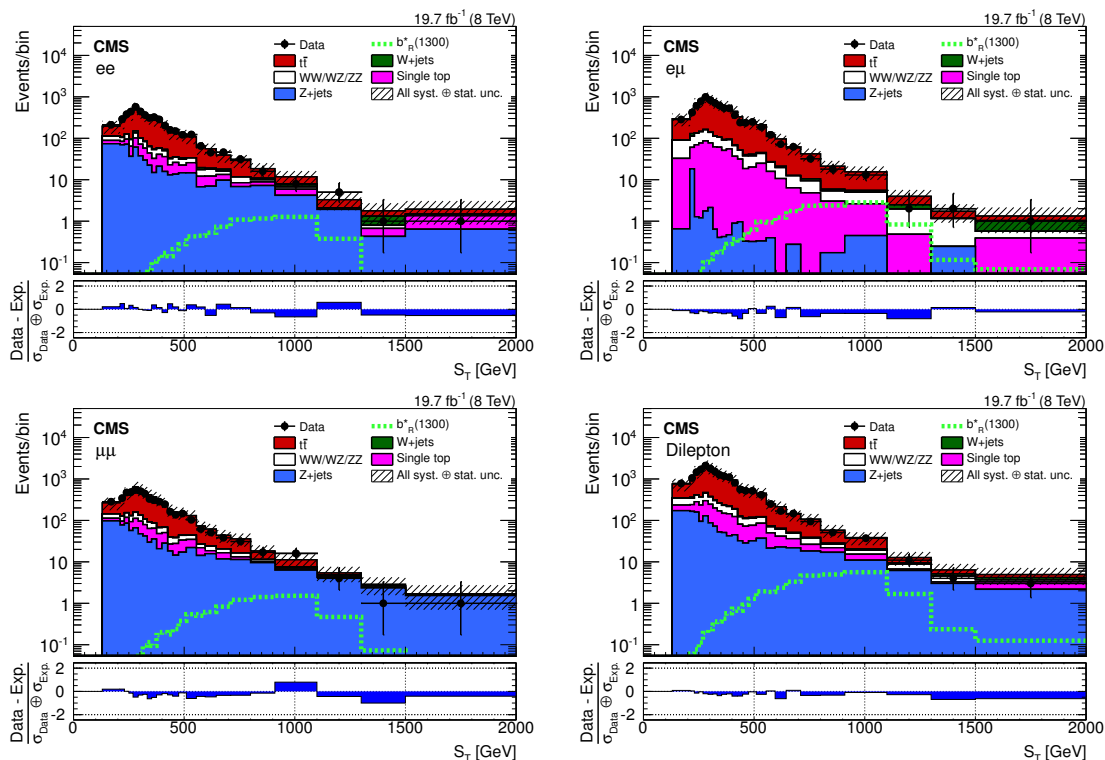**Figure 4**. The S_{T} distribution for data and simulated samples after the event selection is applied, for ee (top left), eμ (top right), $\mu\mu$ (bottom left), and inclusive dilepton (bottom right) channels. The combined statistical and systematic uncertainties are indicated by the hatched band. The bottom plots show the pull ((data-background)$/\sigma_{\mathrm{Data}}\oplus\sigma_{\mathrm{Exp.}}$) between the data and the background estimate distributions. The symbols σ_{Data} and $\sigma_{\mathrm{Exp.}}$ refer to the statistical uncertainty in data, and the systematic uncertainty in the background, respectively.

6 Systematic uncertainties

Systematic uncertainties are divided into four groups: theoretical, background normalization, instrumental, and other measurement-related uncertainties. These uncertainties are summarized in table 5.

6.1 Theoretical uncertainties

Several uncertainties in event simulation are considered. The PDF uncertainties are estimated with the CT10 PDF eigenvector set [21].

In order to estimate uncertainties originating from the top quark mass, additional simulated samples are produced by varying the top quark mass up and down by 5 GeV. A linear extrapolation is applied to scale down the top quark mass uncertainty to 1 GeV. This is applied to $t\bar{t}$ and single top quark t-channel samples. In order to estimate uncertainties originating from the choice of the renormalization and factorization scales (μ_R and μ_F), for the $t\bar{t}$, and single top quark t-channel simulation, the nominal samples use $\mu_R^2 = \mu_F^2 = M_t^2 + \sum p_T^2$ [16], where $\sum p_T^2$ sums over outgoing partons. To evaluate the effect of this scale choice, additional MC samples are produced by varying μ_R and μ_F simultaneously by a factor of 0.5 or 2.0.

Source of uncertainty	Uncertainty	All-hadronic	Lepton+jets	Dilepton
Integrated luminosity	2.6%	⊕	⊕	⊕
$t\bar{t}$ cross section	5.3%		⊕	⊕
$t\bar{t}$ normalization from data	22%	⊙		
Single top quark t-channel σ	15%	⊕	⊕	
Single top quark tW-channel σ	20%	⊕	⊕	⊕
Single top quark s-channel σ	30%	⊕	⊕	
Diboson cross section	30%		⊕	⊕
Z+jets cross section	20%		⊕	⊕
W+jets cross section	8%			⊙
Double lepton triggers	2%			⊙
Dilepton muon ID and isolation	2%			⊙
Dilepton electron ID and isolation	2%			⊙
Dilepton pileup uncertainty	2.6%			⊙
W tagging	8%	⊙		
t tagging	13%	⊙		
Unclustered energy (E_T^{miss} uncertainty)	10%		⊙	
Single-lepton triggers	$\pm 1\sigma(p_T, \eta)$		⊙	
H_T trigger	$\pm 1\sigma(p_{T1} + p_{T2})$	⊙		
Electron ID and isolation	$\pm 1\sigma(p_T, \eta)$		⊙	
Muon ID and isolation	$\pm 1\sigma(p_T, \eta)$		⊙	
Jet energy scale	$\pm 1\sigma(p_T, \eta)$	⊕	⊕	⊕
Jet energy resolution	$\pm 1\sigma(\eta)$	⊕	⊕	⊕
Pileup uncertainty	$\pm 1\sigma$		⊙	
b tagging efficiency	$\pm 1\sigma(p_T, \eta)$		⊙	
b mistagging rate	$\pm 1\sigma(p_T, \eta)$		⊙	
Multijet background	sideband	⊙	⊙	
W+jets background	sideband		⊙	
PDF uncertainty	$\pm 1\sigma$		⊙	
$t\bar{t}$ μ_R and μ_F scales	$4Q^2$ and $0.25Q^2$	⊕	⊕	⊕
Top quark mass	$\pm 1\,\mathrm{GeV}$ for $\mathrm{m_{top}}$		⊙	
Simulation statistical uncertainty		⊙	⊙	⊙

Table 5. Sources of systematic uncertainty for the three analysis channels. For the shape-based uncertainties, the parameterization used for the uncertainty deviation is given in parentheses. Sources marked with "sideband" are measured from data, and contain various uncertainty sources. Uncorrelated uncertainties that apply to a given channel are marked by ⊙. Uncertainties correlated between channels are marked by ⊕. The uncertainties varying as functions of variables in question are indicated if no uncertainty value is listed.

6.2 Background normalization uncertainty

For the lepton+jets and dilepton analysis, the $t\bar{t}$ cross section uncertainty of $\pm 5.3\%$ [46] is used.

The all-hadronic channel extracts the $t\bar{t}$ normalization from data, resulting in an uncertainty of 22% obtained from the fit.

The normalization uncertainties in single top quark t-, tW-, and s-channel cross sections are 15%, 30% and 20%, respectively [23]. The normalization uncertainties in diboson production cross sections are 30%, which is the sum of the experimentally measured cross section uncertainty [47] and uncertainties due to extra jet production. The normalization uncertainty in the Z+jets background is 20%, which is the sum of the experimentally measured cross section uncertainty [48] and uncertainties due to extra jet production. The normalization uncertainty in the W+jets background is 45% for the electron+jets channel and 30% for the muon+jets channel, estimated from data and described in section 5.2. Detector effects and modeling uncertainties that affect the templates are included in the uncertainty.

The normalization uncertainties in the multijet backgrounds are $\pm 33\%$ and $^{+170}_{-100}\%$ for the electron+jets and the muon+jets channels, respectively, estimated from data and described in section 5.2. The uncertainties originating from detector effects, theoretical modeling, and the multijet background control region choice are summed in quadrature to give the uncertainties in the multijet and W+jets background estimations.

6.3 Other measurement uncertainties

In the all-hadronic channel, we correct the simulation by using the trigger efficiency extracted from data that is obtained from a control sample triggered with a lower H_T threshold than in the standard event selection. The scale factors are parameterized as a function of the summed leading and sub-leading jet p_T. To obtain a systematic uncertainty for this correction, we vary the trigger efficiency ϵ by $\pm (1 - \epsilon)/2$, which results in less than a 1% change of the yields for all samples.

The differences between data and simulation due to the electron trigger, identification, and isolation efficiencies are corrected with p_T- and η-dependent scale factors by comparing simulation with a $Z \rightarrow ee$ data sample. The uncertainties due to the statistically limited $Z \rightarrow ee$ samples and the uncertainties in the theoretical inputs to the simulation are taken into account.

The scale factor measurements define the uncertainties for electron trigger, identification, and isolation requirements, and these uncertainties are less than 1%. Scale factors related to the muon trigger, identification, and isolation efficiency are measured in a similar way to those for electrons, but use $Z \rightarrow \mu\mu$, where the uncertainties are less than 2% [49], instead of $Z \rightarrow ee$ events.

The jet energy resolution [50] systematic uncertainty is an η-dependent smearing of the jet energy resolution for simulated events, which results in a less than 0.4% acceptance change. The jet energy scale [50] systematic uncertainty is parameterized in p_T and η and applied to simulated samples to cover the difference between data and simulation, which is typically 5% or less. The all-hadronic channel has an additional 3% uncertainty because the jet energy scale is measured from anti-k_T jets, but applied to CA jets. The jet energy scale

uncertainty is propagated in the $E_{\mathrm{T}}^{\mathrm{miss}}$ calculation. The estimation of $E_{\mathrm{T}}^{\mathrm{miss}}$ includes an additional uncertainty due to the effect of unclustered energy arising from the jets or leptons.

The b tagging efficiency and mistagging rate uncertainty are estimated by comparing a b jet enriched μ+jets data sample with simulation [44]. The differences are corrected by jet flavor (b jet, c jet, and light jets from u/d/s/gluon), p_{T}- and η-dependent b tagging and mistagging scale factors. The uncertainties in these scale factors are propagated to the b tagging event weight calculation independently, giving the uncertainties in b tagging efficiency and mistagging rate. The typical acceptance change due to b tagging efficiency is less than 3%. The mistagging rate brings about an uncertainty of 0.3% for samples that have at least one b jet and of 9.0% for samples that have no b jets. The all-hadronic channel includes a 13% uncertainty in the t tagging scale factor, which is used to correct for differences in subjet identification efficiencies between data and simulation [45].

The result of a polynomial fit to the t mistagging rate extracted from a control region as a function of jet p_{T} is applied to events before applying the t tagging algorithm to estimate the multijet background contribution in the all-hadronic channel. The fit introduces a 9% statistical uncertainty and a 12% uncertainty to allow for the possibility of choosing alternative functional forms. There is a difference between the shape of the jet mass distribution of the top quark candidate in the control and signal regions. This is corrected by a top quark jet mass dependent weight derived from the multijet simulation. This correction contributes an extra 0.3% uncertainty in the total multijet yield. The uncertainty due to the choice of parameterization in the t mistagging rate is taken to be the difference between a parameterization in p_{T}, η and a parameterization in p_{T}, η, m_{tW}. This difference is about 2% of the total multijet yield, with an additional 20% statistical uncertainty from the higher dimensional parameterization.

To estimate the uncertainty due to pileup modeling in simulation, we vary the measured minimum bias cross section of 69.4 mb by $\pm5\%$. These variations are then propagated to analysis results by modifying the pileup multiplicity accordingly [51]. The uncertainty in the integrated luminosity is measured in dedicated samples and applied to the signal and backgrounds based on simulation. The size of this uncertainty is 2.6% [52].

7 Results and interpretation

A binned maximum likelihood fit to the m_{tW} distribution is performed in both the all-hadronic and lepton+jets channels, and to the S_{T} distribution in the dilepton channel to extract the signal cross section. The observed distributions are consistent with those from the background only prediction. A Bayesian method [12, Ch. 38] with a flat signal prior is used within the THETA framework [53] to set limits on $\sigma_{\mathrm{gb}\to\mathrm{b}^*\to\mathrm{tW}}$. The systematic uncertainties are accounted for as nuisance parameters, and are integrated out using Bayesian marginalization. Rate uncertainties are modeled using log-normal priors. Uncertainties varying as functions of the fitted variables are modeled using Gaussian priors, and template morphing is employed to model the shape of these systematic uncertainties. The limits on the cross section times branching fraction ($\sigma_{\mathrm{gb}\to\mathrm{b}^*\to\mathrm{tW}}$) at 95% confidence level (CL) are shown in figures 5, 6, and 7 for the all-hadronic, lepton+jets, and dilepton channels, respectively.
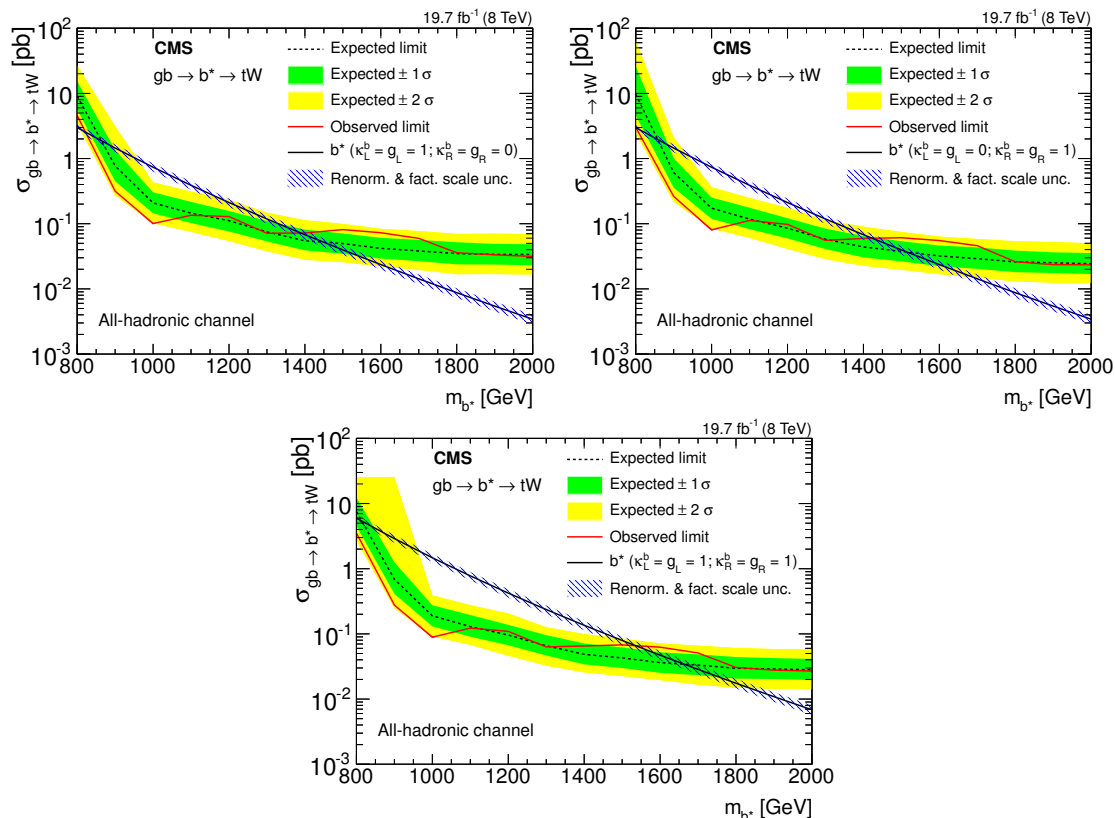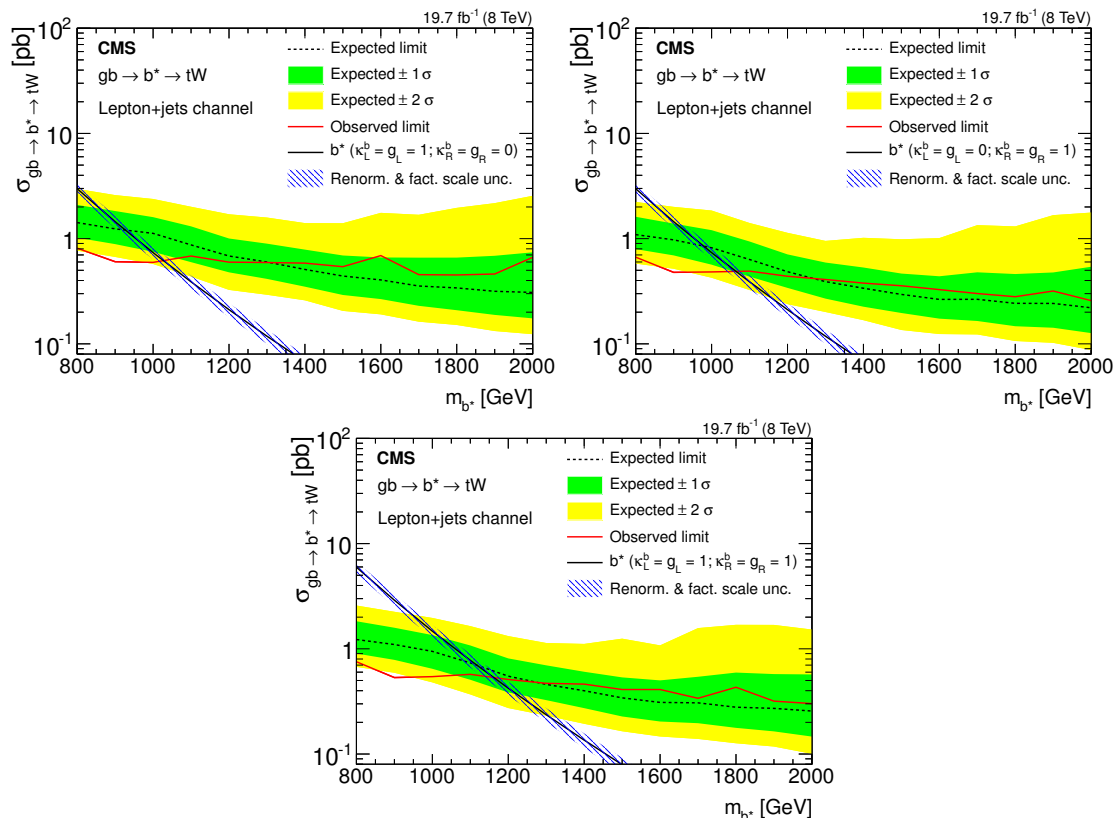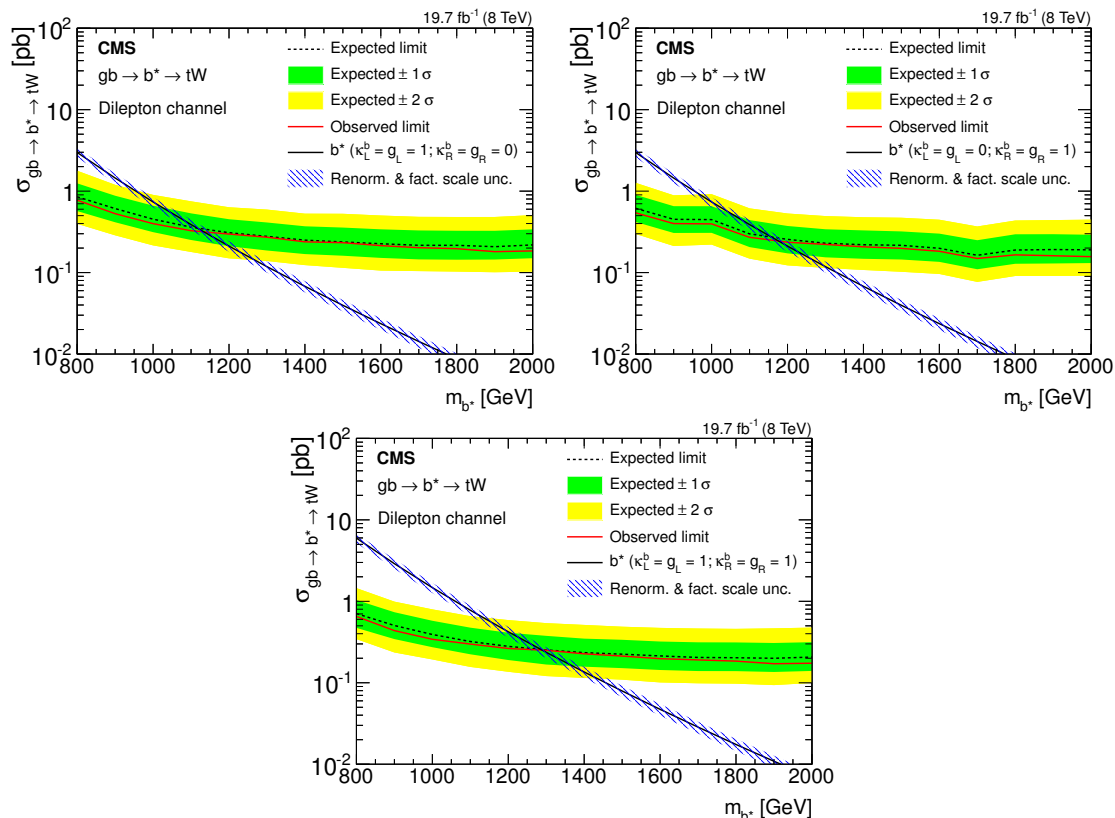
Figure 5. The expected (dashed) and observed (solid) production cross section limits at 95% CL for the all-hadronic channel as a function of b* quark mass for gb → b* → tW. The theoretical cross section (solid line with hatched area) is also shown for comparison. The 1σ and 2σ uncertainties in the expected limit bands are shown. Limits for the left-handed, right-handed, and vector-like b* quark coupling hypotheses are shown in the top left, top right, and bottom plots, respectively.

To enhance the sensitivity of the measurement of the upper limit on the gb → b* → tW production cross section, the all-hadronic, lepton+jets, and dilepton channels are combined. In forming the combination of separate channels, systematic uncertainties affecting both the shape and the event yield are taken into account. The procedure adopted is as follows: for each channel the shape of each distribution is determined and the normalization is set to 1. Then, for each bin "i", an estimate is made of the systematic uncertainty σ_i (not necessarily symmetric), which takes into account the contributions from all the sources affecting the shape. "Upper" and "lower" distributions are then obtained, each normalized to unity, and used to estimate event yields in two limiting cases. The systematic uncertainties are treated as being completely correlated between bins of the distribution, while the statistical uncertainties are treated as uncorrelated. In the combination, the uncertainty sources due to jet energy scale, jet energy resolution, b tagging scale factor, single top quark cross section, and integrated luminosity are treated as correlated, and the remaining uncertainties are assumed to be uncorrelated, as shown in table 5. The limits are shown in figure 8. The expected (observed) mass exclusion region at 95% CL for the left-handed,
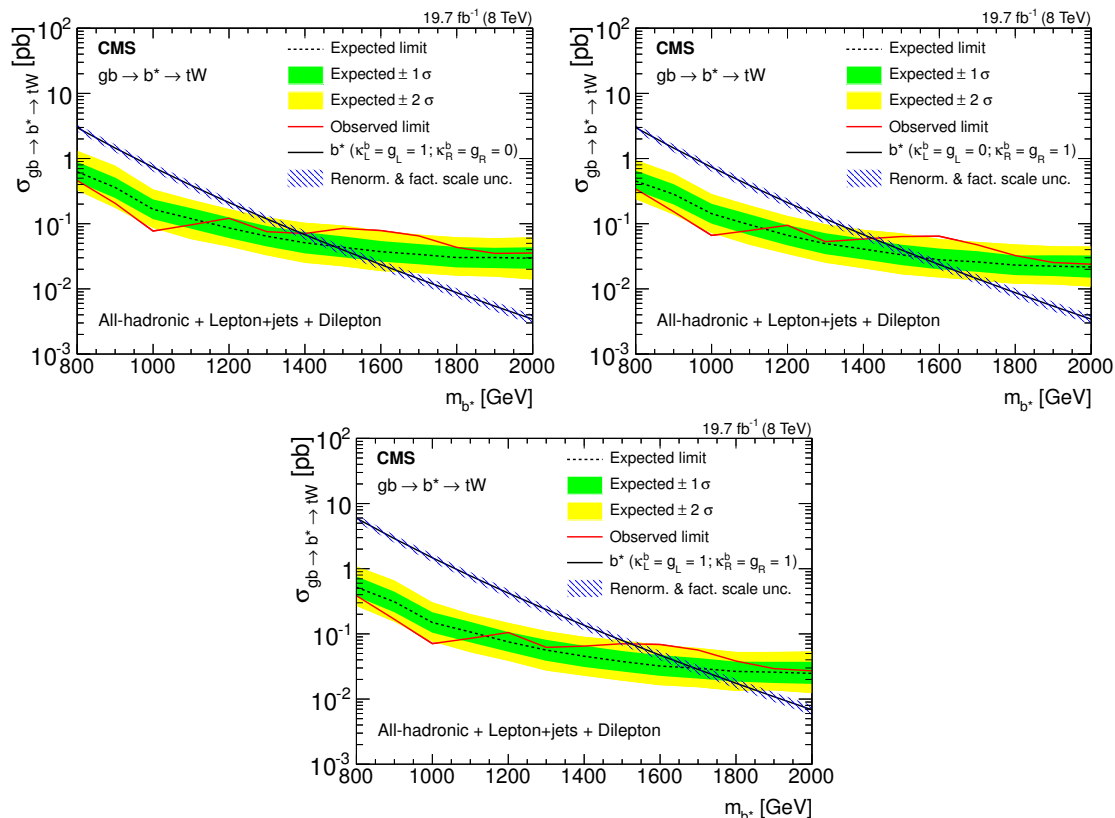
Figure 6. The expected (dashed) and observed (solid) production cross section limits at 95% CL for the lepton+jets channel as a function of b* quark mass for $gb \to b^* \to tW$. The theoretical cross section (solid line with hatched area) is also shown for comparison. The 1σ and 2σ uncertainties in the expected limit bands are shown. Limits for the left-handed, right-handed, and vector-like b* quark coupling hypotheses are shown in the top left, top right, and bottom plots, respectively.

right-handed, and vector-like b* quark hypotheses is below 1480, 1560, and 1690 GeV (1390, 1430, and 1530 GeV), respectively as summarized in table 6.

The upper limits on the cross section times branching fraction may be generalized as a function of the couplings κ and g, defined in equations (1.1) and (1.2). The results are shown in figure 9.

8 Summary

A search for a singly produced b* quark decaying to tW in the all-hadronic, lepton+jets, and dilepton final states has been performed using proton-proton collisions recorded by the CMS detector at $\sqrt{s} = 8$ TeV, corresponding to an integrated luminosity of 19.7 fb^{-1}. No deviations that are inconsistent with standard model expectations are found in the various spectra of variables used to search for the signal in the three channels. Upper limits are set at 95% confidence level on the product of cross section and branching fraction for the production of a b* quark that subsequently decays to tW. Excited bottom quarks are excluded with masses below 1390, 1430, and 1530 GeV for left-handed, right-handed, and

Figure 7. The expected (dashed) and observed (solid) production cross section limits at 95% CL for the dilepton channel as a function of b* quark mass for gb → b* → tW. The theoretical cross section (solid line with hatched area) is also shown for comparison. The 1σ and 2σ uncertainties in the expected limit bands are shown. Limits for the left-handed, right-handed, and vector-like b* quark coupling hypotheses are shown in the top left, top right, and bottom plots, respectively.

vector-like b* quark couplings, respectively. The mass limits are also extrapolated to the two dimensional κ-g coupling plane. These are the most stringent limits on the b* quark masses to date.

Acknowledgments

Figure 8. The expected (dashed) and observed (solid) production cross section limits at 95% CL for the combined all-hadronic, lepton+jets, and dilepton channels as a function of b^* quark mass for $gb \to b^* \to tW$. The theoretical cross section (solid line with hatched area) is also shown for comparison. The 1σ and 2σ uncertainties in the expected limit bands are shown. Limits for the left-handed, right-handed, and vector-like b^* quark coupling hypotheses are shown in the top left, top right, and bottom plots, respectively.
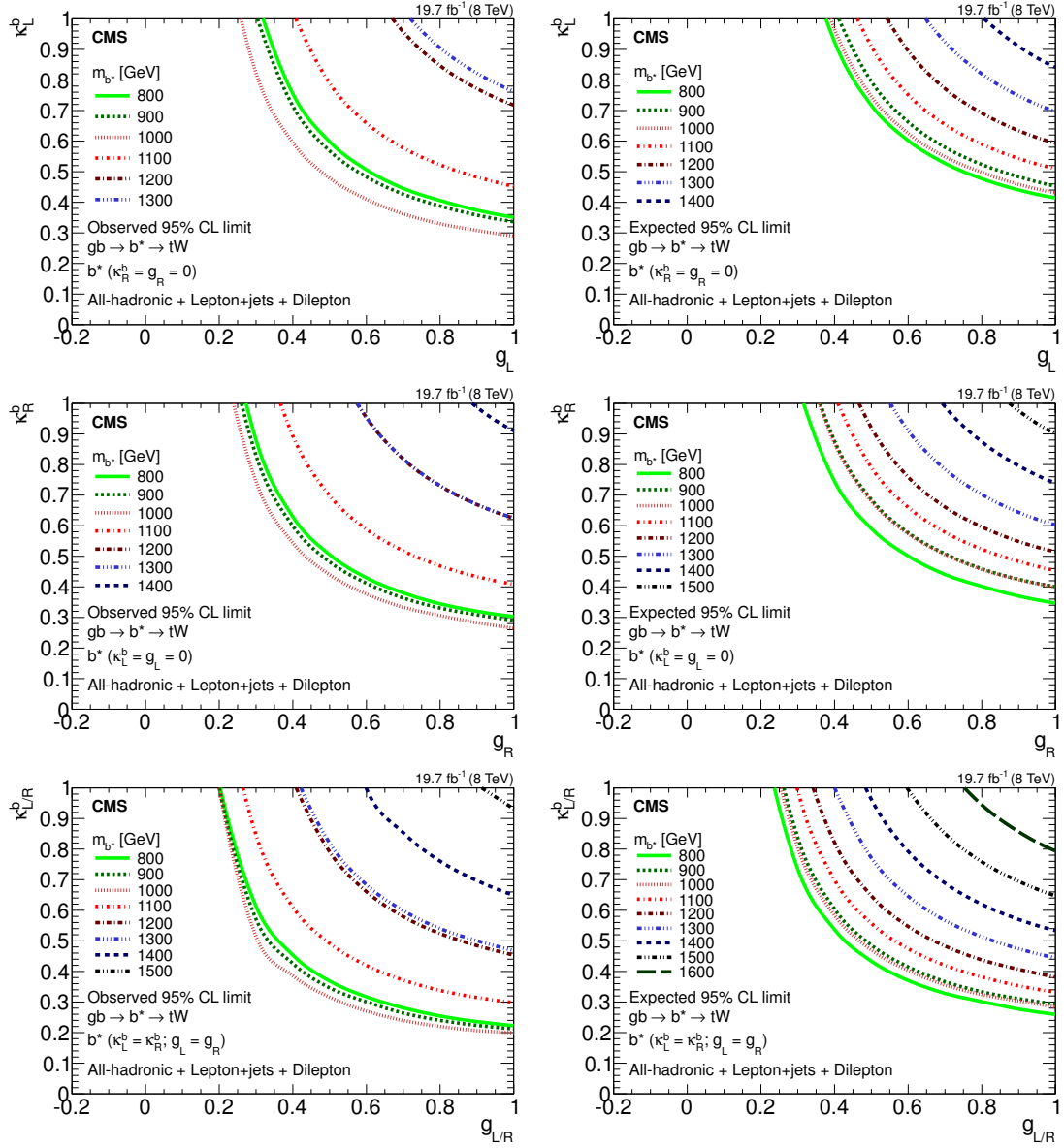
Figure 9. Contour plots showing the lower limits on various values of the b* quark mass, as a function of the couplings κ and g. The left column shows the observed limits and the right column shows the expected limits. The limits for the left-handed, right-handed, and vector-like b* quark coupling hypotheses are shown in the top, middle, and bottom rows, respectively. The excluded regions are above and to the right of the curves.

	Left-handed	Right-handed	Vector-like
All-hadronic channel			
Expected 95% CL limit [GeV]	890 - 1460	889 - 1520	842 - 1670
Observed 95% CL limit [GeV]	858 - 1390	803 - 1430	1540
Lepton+jets channel			
Expected 95% CL limit [GeV]	935	985	1130
Observed 95% CL limit [GeV]	1030	1070	1170
Dilepton channel			
Expected 95% CL limit [GeV]	1120	1170	1290
Observed 95% CL limit [GeV]	1140	1180	1290
All-hadronic, lepton+jets, and dilepton channels combined			
Expected 95% CL limit [GeV]	1480	1560	1690
Observed 95% CL limit [GeV]	1390	1430	1530

Table 6. The limit at 95% CL, for the case of unit couplings, on b* quark mass for the left-handed, right-handed, and vector-like coupling hypotheses in the all-hadronic, lepton+jets dilepton, and combined channels. For each domain, two numbers linked with a dash indicate the excluded b* quark mass range, a single number indicates the excluded lower b* quark mass limit.

References

[1] ATLAS collaboration, *Observation of a new particle in the search for the standard model Higgs boson with the ATLAS detector at the LHC*, *Phys. Lett.* **B 716** (2012) 1 [`arXiv:1207.7214`] [ɪɴSPIRE].

[2] CMS collaboration, *Observation of a new boson at a mass of* 125 *GeV with the CMS experiment at the LHC*, *Phys. Lett.* **B 716** (2012) 30 [`arXiv:1207.7235`] [ɪɴSPIRE].

[3] CMS collaboration, *Observation of a new boson with mass near* 125 *GeV in pp collisions at* $\sqrt{s} = 7$ *and* 8 *TeV*, *JHEP* **06** (2013) 081 [`arXiv:1303.4571`] [ɪɴSPIRE].

[4] C. Cheung, A.L. Fitzpatrick and L. Randall, *Sequestering CP-violation and GIM-violation with warped extra dimensions*, *JHEP* **01** (2008) 069 [`arXiv:0711.4421`] [ɪɴSPIRE].

[5] A.L. Fitzpatrick, G. Perez and L. Randall, *Flavor anarchy in a Randall-Sundrum model with* 5*D minimal flavor violation and a low Kaluza-Klein scale*, *Phys. Rev. Lett.* **100** (2008) 171604 [`arXiv:0710.1869`] [ɪɴSPIRE].

[6] C. Bini, R. Contino and N. Vignaroli, *Heavy-light decay topologies as a new strategy to discover a heavy gluon*, *JHEP* **01** (2012) 157 [`arXiv:1110.6058`] [ɪɴSPIRE].

[7] N. Vignaroli, *Discovering the composite Higgs through the decay of a heavy fermion*, *JHEP* **07** (2012) 158 [`arXiv:1204.0468`] [ɪɴSPIRE].

[8] N. Vignaroli, $\Delta F = 1$ *constraints on composite Higgs models with LR parity*, *Phys. Rev.* **D 86** (2012) 115011 [`arXiv:1204.0478`] [ɪɴSPIRE].

[9] ATLAS collaboration, *ATLAS search for new phenomena in dijet mass and angular distributions using pp collisions at* $\sqrt{s} = 7$ *TeV*, *JHEP* **01** (2013) 029 [`arXiv:1210.1718`] [ɪɴSPIRE].

[10] CMS collaboration, *Search for resonances and quantum black holes using dijet mass spectra in proton-proton collisions at* $\sqrt{s} = 8$ *TeV*, *Phys. Rev.* **D 91** (2015) 052009 [`arXiv:1501.04198`] [ɪɴSPIRE].

[11] ATLAS collaboration, *Search for single b^*-quark production with the ATLAS detector at* $\sqrt{s} = 7$ *TeV*, *Phys. Lett.* **B 721** (2013) 171 [arXiv:1301.1583] [INSPIRE].

[12] PARTICLE DATA GROUP collaboration, K.A. Olive et al., *Review of particle physics*, *Chin. Phys.* **C 38** (2014) 090001 [INSPIRE].

[13] U. Baur, M. Spira and P.M. Zerwas, *Excited quark and lepton production at hadron colliders*, *Phys. Rev.* **D 42** (1990) 815 [INSPIRE].

[14] J. Nutter, R. Schwienhorst, D.G.E. Walker and J.-H. Yu, *Single top production as a probe of* B' *quarks*, *Phys. Rev.* **D 86** (2012) 094006 [arXiv:1207.5179] [INSPIRE].

[15] CMS collaboration, *The CMS experiment at the CERN LHC*, 2008 *JINST* **3** S08004 [INSPIRE].

[16] J. Alwall et al., *The automated computation of tree-level and next-to-leading order differential cross sections and their matching to parton shower simulations*, *JHEP* **07** (2014) 079 [arXiv:1405.0301] [INSPIRE].

[17] J. Pumplin, D.R. Stump, J. Huston, H.L. Lai, P.M. Nadolsky and W.K. Tung, *New generation of parton distributions with uncertainties from global QCD analysis*, *JHEP* **07** (2002) 012 [hep-ph/0201195] [INSPIRE].

[18] P. Nason, *A new method for combining NLO QCD with shower Monte Carlo algorithms*, *JHEP* **11** (2004) 040 [hep-ph/0409146] [INSPIRE].

[19] S. Frixione, P. Nason and C. Oleari, *Matching NLO QCD computations with parton shower simulations: the POWHEG method*, *JHEP* **11** (2007) 070 [arXiv:0709.2092] [INSPIRE].

[20] S. Alioli, P. Nason, C. Oleari and E. Re, *A general framework for implementing NLO calculations in shower Monte Carlo programs: the POWHEG BOX*, *JHEP* **06** (2010) 043 [arXiv:1002.2581] [INSPIRE].

[21] H.-L. Lai et al., *New parton distributions for collider physics*, *Phys. Rev.* **D 82** (2010) 074024 [arXiv:1007.2241] [INSPIRE].

[22] M. Czakon, P. Fiedler and A. Mitov, *Total top-quark pair-production cross section at hadron colliders through* $O(\alpha_S^4)$, *Phys. Rev. Lett.* **110** (2013) 252004 [arXiv:1303.6254] [INSPIRE].

[23] N. Kidonakis, *Differential and total cross sections for top pair and single top production*, arXiv:1205.3453 [INSPIRE].

[24] R. Gavin, Y. Li, F. Petriello and S. Quackenbush, *FEWZ 2.0: a code for hadronic Z production at next-to-next-to-leading order*, *Comput. Phys. Commun.* **182** (2011) 2388 [arXiv:1011.3540] [INSPIRE].

[25] T. Sjöstrand, S. Mrenna and P.Z. Skands, *PYTHIA 6.4 physics and manual*, *JHEP* **05** (2006) 026 [hep-ph/0603175] [INSPIRE].

[26] J.M. Campbell and R.K. Ellis, *MCFM for the Tevatron and the LHC*, *Nucl. Phys. Proc. Suppl.* **205-206** (2010) 10 [arXiv:1007.3492] [INSPIRE].

[27] CMS collaboration, *Measurement of the underlying event activity at the LHC with* $\sqrt{s} = 7$ *TeV and comparison with* $\sqrt{s} = 0.9$ *TeV*, *JHEP* **09** (2011) 109 [arXiv:1107.0330] [INSPIRE].

[28] GEANT4 collaboration, S. Agostinelli et al., *GEANT4: a simulation toolkit*, *Nucl. Instrum. Meth.* **A 506** (2003) 250 [INSPIRE].

[29] CMS collaboration, *Description and performance of track and primary-vertex reconstruction with the CMS tracker*, 2014 *JINST* **9** P10009 [arXiv:1405.6569] [INSPIRE].

[30] CMS collaboration, *Particle-flow event reconstruction in CMS and performance for jets, taus and MET*, CMS-PAS-PFT-09-001, CERN, Geneva Switzerland (2009).

[31] CMS collaboration, *Performance of electron reconstruction and selection with the CMS detector in proton-proton collisions at $\sqrt{s} = 8\,TeV$*, 2015 *JINST* **10** P06005 [arXiv:1502.02701] [INSPIRE].

[32] CMS collaboration, *Pileup jet identification*, CMS-PAS-JME-13-005, CERN, Geneva Switzerland (2013).

[33] CMS collaboration, *The performance of the CMS muon detector in proton-proton collisions at $\sqrt{s} = 7\,TeV$ at the LHC*, 2013 *JINST* **8** P11002 [arXiv:1306.6905] [INSPIRE].

[34] M. Cacciari, G.P. Salam and G. Soyez, *The anti-k_t jet clustering algorithm*, *JHEP* **04** (2008) 063 [arXiv:0802.1189] [INSPIRE].

[35] M. Cacciari, G.P. Salam and G. Soyez, *FastJet user manual*, *Eur. Phys. J.* **C 72** (2012) 1896 [arXiv:1111.6097] [INSPIRE].

[36] M. Cacciari and G.P. Salam, *Pileup subtraction using jet areas*, *Phys. Lett.* **B 659** (2008) 119 [arXiv:0707.1378] [INSPIRE].

[37] CMS collaboration, *Identification of b-quark jets with the CMS experiment*, 2013 *JINST* **8** P04013 [arXiv:1211.4462] [INSPIRE].

[38] Y.L. Dokshitzer, G.D. Leder, S. Moretti and B.R. Webber, *Better jet clustering algorithms*, *JHEP* **08** (1997) 001 [hep-ph/9707323] [INSPIRE].

[39] J. Thaler and K. Van Tilburg, *Maximizing boosted top identification by minimizing N-subjettiness*, *JHEP* **02** (2012) 093 [arXiv:1108.2701] [INSPIRE].

[40] S.D. Ellis, C.K. Vermilion and J.R. Walsh, *Techniques for improved heavy particle searches with jet substructure*, *Phys. Rev.* **D 80** (2009) 051501 [arXiv:0903.5081] [INSPIRE].

[41] CMS collaboration, *Identification techniques for highly boosted W bosons that decay into hadrons*, *JHEP* **12** (2014) 017 [arXiv:1410.4227] [INSPIRE].

[42] D.E. Kaplan, K. Rehermann, M.D. Schwartz and B. Tweedie, *Top tagging: a method for identifying boosted hadronically decaying top quarks*, *Phys. Rev. Lett.* **101** (2008) 142001 [arXiv:0806.0848] [INSPIRE].

[43] CMS collaboration, *A Cambridge-Aachen (C-A) based jet algorithm for boosted top-jet tagging*, CMS-PAS-JME-09-001, CERN, Geneva Switzerland (2009).

[44] CMS collaboration, *Performance of b tagging at $\sqrt{s} = 8\,TeV$ in multijet, $t\bar{t}$ and boosted topology events*, CMS-PAS-BTV-13-001, CERN, Geneva Switzerland (2013).

[45] CMS collaboration, *Boosted top jet tagging at CMS*, CMS-PAS-JME-13-007, CERN, Geneva Switzerland (2013).

[46] CMS collaboration, *Measurement of the $t\bar{t}$ production cross section in the dilepton channel in pp collisions at $\sqrt{s} = 8\,TeV$*, *JHEP* **02** (2014) 024 [*Erratum ibid.* **02** (2014) 102] [arXiv:1312.7582] [INSPIRE].

[47] CMS collaboration, *Measurement of W^+W^- and ZZ production cross sections in pp collisions at $\sqrt{s} = 8\,TeV$*, *Phys. Lett.* **B 721** (2013) 190 [arXiv:1301.4698] [INSPIRE].

[48] CMS collaboration, *Measurement of inclusive W and Z boson production cross sections in pp collisions at* $\sqrt{s} = 8$ *TeV*, *Phys. Rev. Lett.* **112** (2014) 191802 [`arXiv:1402.0923`] [INSPIRE].

[49] CMS collaboration, *Performance of CMS muon reconstruction in pp collision events at* $\sqrt{s} = 7$ *TeV*, 2012 *JINST* **7** P10002 [`arXiv:1206.4071`] [INSPIRE].

[50] CMS collaboration, *Determination of jet energy calibration and transverse momentum resolution in CMS*, 2011 *JINST* **6** P11002 [`arXiv:1107.4277`] [INSPIRE].

[51] CMS collaboration, *Measurement of the inelastic proton-proton cross section at* $\sqrt{s} = 7$ *TeV*, *Phys. Lett.* **B 722** (2013) 5 [`arXiv:1210.6718`] [INSPIRE].

[52] CMS collaboration, *CMS luminosity based on pixel cluster counting — summer* 2013 *update*, CMS-PAS-LUM-13-001, CERN, Geneva Switzerland (2013).

[53] J. Ott, *The theta package*, http://www.theta-framework.org/.

The CMS collaboration

Yerevan Physics Institute, Yerevan, Armenia

V. Khachatryan, A.M. Sirunyan, A. Tumasyan

Institut für Hochenergiephysik der OeAW, Wien, Austria

W. Adam, E. Asilar, T. Bergauer, J. Brandstetter, E. Brondolin, M. Dragicevic, J. Erö, M. Flechl, M. Friedl, R. Frühwirth[1], V.M. Ghete, C. Hartl, N. Hörmann, J. Hrubec, M. Jeitler[1], V. Knünz, A. König, M. Krammer[1], I. Krätschmer, D. Liko, T. Matsushita, I. Mikulec, D. Rabady[2], B. Rahbaran, H. Rohringer, J. Schieck[1], R. Schöfbeck, J. Strauss, W. Treberer-Treberspurg, W. Waltenberger, C.-E. Wulz[1]

National Centre for Particle and High Energy Physics, Minsk, Belarus

V. Mossolov, N. Shumeiko, J. Suarez Gonzalez

Universiteit Antwerpen, Antwerpen, Belgium

S. Alderweireldt, T. Cornelis, E.A. De Wolf, X. Janssen, A. Knutsson, J. Lauwers, S. Luyckx, S. Ochesanu, R. Rougny, M. Van De Klundert, H. Van Haevermaet, P. Van Mechelen, N. Van Remortel, A. Van Spilbeeck

Vrije Universiteit Brussel, Brussel, Belgium

S. Abu Zeid, F. Blekman, J. D'Hondt, N. Daci, I. De Bruyn, K. Deroover, N. Heracleous, J. Keaveney, S. Lowette, L. Moreels, A. Olbrechts, Q. Python, D. Strom, S. Tavernier, W. Van Doninck, P. Van Mulders, G.P. Van Onsem, I. Van Parijs

Université Libre de Bruxelles, Bruxelles, Belgium

P. Barria, C. Caillol, B. Clerbaux, G. De Lentdecker, H. Delannoy, G. Fasanella, L. Favart, A.P.R. Gay, A. Grebenyuk, G. Karapostoli, T. Lenzi, A. Léonard, T. Maerschalk, A. Marinov, L. Perniè, A. Randle-conde, T. Reis, T. Seva, C. Vander Velde, P. Vanlaer, R. Yonamine, F. Zenoni, F. Zhang[3]

Ghent University, Ghent, Belgium

K. Beernaert, L. Benucci, A. Cimmino, S. Crucy, D. Dobur, A. Fagot, G. Garcia, M. Gul, J. Mccartin, A.A. Ocampo Rios, D. Poyraz, D. Ryckbosch, S. Salva, M. Sigamani, N. Strobbe, M. Tytgat, W. Van Driessche, E. Yazgan, N. Zaganidis

Université Catholique de Louvain, Louvain-la-Neuve, Belgium

S. Basegmez, C. Beluffi[4], O. Bondu, S. Brochet, G. Bruno, R. Castello, A. Caudron, L. Ceard, G.G. Da Silveira, C. Delaere, D. Favart, L. Forthomme, A. Giammanco[5], J. Hollar, A. Jafari, P. Jez, M. Komm, V. Lemaitre, A. Mertens, C. Nuttens, L. Perrini, A. Pin, K. Piotrzkowski, A. Popov[6], L. Quertenmont, M. Selvaggi, M. Vidal Marono

Université de Mons, Mons, Belgium

N. Beliy, G.H. Hammad

Centro Brasileiro de Pesquisas Fisicas, Rio de Janeiro, Brazil

W.L. Aldá Júnior, G.A. Alves, L. Brito, M. Correa Martins Junior, M. Hamer, C. Hensel, C. Mora Herrera, A. Moraes, M.E. Pol, P. Rebello Teles

Universidade do Estado do Rio de Janeiro, Rio de Janeiro, Brazil

E. Belchior Batista Das Chagas, W. Carvalho, J. Chinellato[7], A. Custódio, E.M. Da Costa, D. De Jesus Damiao, C. De Oliveira Martins, S. Fonseca De Souza, L.M. Huertas Guativa, H. Malbouisson, D. Matos Figueiredo, L. Mundim, H. Nogima, W.L. Prado Da Silva, A. Santoro, A. Sznajder, E.J. Tonelli Manganote[7], A. Vilela Pereira

Universidade Estadual Paulista [a]**, Universidade Federal do ABC** [b]**, São Paulo, Brazil**

S. Ahuja[a], C.A. Bernardes[b], A. De Souza Santos[b], S. Dogra[a], T.R. Fernandez Perez Tomei[a], E.M. Gregores[b], P.G. Mercadante[b], C.S. Moon[a,8], S.F. Novaes[a], Sandra S. Padula[a], D. Romero Abad, J.C. Ruiz Vargas

Institute for Nuclear Research and Nuclear Energy, Sofia, Bulgaria

A. Aleksandrov, R. Hadjiiska, P. Iaydjiev, M. Rodozov, S. Stoykova, G. Sultanov, M. Vutova

University of Sofia, Sofia, Bulgaria

A. Dimitrov, I. Glushkov, L. Litov, B. Pavlov, P. Petkov

Institute of High Energy Physics, Beijing, China

M. Ahmad, J.G. Bian, G.M. Chen, H.S. Chen, M. Chen, T. Cheng, R. Du, C.H. Jiang, F. Romeo, S.M. Shaheen, J. Tao, C. Wang, Z. Wang, H. Zhang, S. Zhu

State Key Laboratory of Nuclear Physics and Technology, Peking University, Beijing, China

C. Asawatangtrakuldee, Y. Ban, Q. Li, S. Liu, Y. Mao, S.J. Qian, D. Wang, Z. Xu, W. Zou

Universidad de Los Andes, Bogota, Colombia

C. Avila, A. Cabrera, L.F. Chaparro Sierra, C. Florez, J.P. Gomez, B. Gomez Moreno, J.C. Sanabria

University of Split, Faculty of Electrical Engineering, Mechanical Engineering and Naval Architecture, Split, Croatia

N. Godinovic, D. Lelas, I. Puljak, P.M. Ribeiro Cipriano

University of Split, Faculty of Science, Split, Croatia

Z. Antunovic, M. Kovac

Institute Rudjer Boskovic, Zagreb, Croatia

V. Brigljevic, K. Kadija, J. Luetic, S. Micanovic, L. Sudic

University of Cyprus, Nicosia, Cyprus

A. Attikis, G. Mavromanolakis, J. Mousa, C. Nicolaou, F. Ptochos, P.A. Razis, H. Rykaczewski

Charles University, Prague, Czech Republic

M. Bodlak, M. Finger[9], M. Finger Jr.[9]

Academy of Scientific Research and Technology of the Arab Republic of Egypt, Egyptian Network of High Energy Physics, Cairo, Egypt

A. Awad[10,11], E. El-khateeb[10], A. Mohamed[12], E. Salama[10,11]

National Institute of Chemical Physics and Biophysics, Tallinn, Estonia

B. Calpas, M. Kadastik, M. Murumaa, M. Raidal, A. Tiko, C. Veelken

Department of Physics, University of Helsinki, Helsinki, Finland

P. Eerola, J. Pekkanen, M. Voutilainen

Helsinki Institute of Physics, Helsinki, Finland

J. Härkönen, V. Karimäki, R. Kinnunen, T. Lampén, K. Lassila-Perini, S. Lehti, T. Lindén, P. Luukka, T. Mäenpää, T. Peltola, E. Tuominen, J. Tuominiemi, E. Tuovinen, L. Wendland

Lappeenranta University of Technology, Lappeenranta, Finland

J. Talvitie, T. Tuuva

DSM/IRFU, CEA/Saclay, Gif-sur-Yvette, France

M. Besancon, F. Couderc, M. Dejardin, D. Denegri, B. Fabbro, J.L. Faure, C. Favaro, F. Ferri, S. Ganjour, A. Givernaud, P. Gras, G. Hamel de Monchenault, P. Jarry, E. Locci, M. Machet, J. Malcles, J. Rander, A. Rosowsky, M. Titov, A. Zghiche

Laboratoire Leprince-Ringuet, Ecole Polytechnique, IN2P3-CNRS, Palaiseau, France

I. Antropov, S. Baffioni, F. Beaudette, P. Busson, L. Cadamuro, E. Chapon, C. Charlot, T. Dahms, O. Davignon, N. Filipovic, A. Florent, R. Granier de Cassagnac, S. Lisniak, L. Mastrolorenzo, P. Miné, I.N. Naranjo, M. Nguyen, C. Ochando, G. Ortona, P. Paganini, S. Regnard, R. Salerno, J.B. Sauvan, Y. Sirois, T. Strebler, Y. Yilmaz, A. Zabi

Institut Pluridisciplinaire Hubert Curien, Université de Strasbourg, Université de Haute Alsace Mulhouse, CNRS/IN2P3, Strasbourg, France

J.-L. Agram[13], J. Andrea, A. Aubin, D. Bloch, J.-M. Brom, M. Buttignol, E.C. Chabert, N. Chanon, C. Collard, E. Conte[13], X. Coubez, J.-C. Fontaine[13], D. Gelé, U. Goerlach, C. Goetzmann, A.-C. Le Bihan, J.A. Merlin[2], K. Skovpen, P. Van Hove

Centre de Calcul de l'Institut National de Physique Nucleaire et de Physique des Particules, CNRS/IN2P3, Villeurbanne, France

S. Gadrat

Université de Lyon, Université Claude Bernard Lyon 1, CNRS-IN2P3, Institut de Physique Nucléaire de Lyon, Villeurbanne, France

S. Beauceron, C. Bernet, G. Boudoul, E. Bouvier, C.A. Carrillo Montoya, J. Chasserat, R. Chierici, D. Contardo, B. Courbon, P. Depasse, H. El Mamouni, J. Fan, J. Fay, S. Gascon, M. Gouzevitch, B. Ille, F. Lagarde, I.B. Laktineh, M. Lethuillier, L. Mirabito, A.L. Pequegnot, S. Perries, J.D. Ruiz Alvarez, D. Sabes, L. Sgandurra, V. Sordini, M. Vander Donckt, P. Verdier, S. Viret, H. Xiao

Georgian Technical University, Tbilisi, Georgia

T. Toriashvili[14]

Tbilisi State University, Tbilisi, Georgia

Z. Tsamalaidze[9]

RWTH Aachen University, I. Physikalisches Institut, Aachen, Germany

C. Autermann, S. Beranek, M. Edelhoff, L. Feld, A. Heister, M.K. Kiesel, K. Klein, M. Lipinski, A. Ostapchuk, M. Preuten, F. Raupach, S. Schael, J.F. Schulte, T. Verlage, H. Weber, B. Wittmer, V. Zhukov[6]

RWTH Aachen University, III. Physikalisches Institut A, Aachen, Germany

M. Ata, M. Brodski, E. Dietz-Laursonn, D. Duchardt, M. Endres, M. Erdmann, S. Erdweg, T. Esch, R. Fischer, A. Güth, T. Hebbeker, C. Heidemann, K. Hoepfner, D. Klingebiel, S. Knutzen, P. Kreuzer, M. Merschmeyer, A. Meyer, P. Millet, M. Olschewski, K. Padeken, P. Papacz, T. Pook, M. Radziej, H. Reithler, M. Rieger, F. Scheuch, L. Sonnenschein, D. Teyssier, S. Thüer

RWTH Aachen University, III. Physikalisches Institut B, Aachen, Germany

V. Cherepanov, Y. Erdogan, G. Flügge, H. Geenen, M. Geisler, F. Hoehle, B. Kargoll, T. Kress, Y. Kuessel, A. Künsken, J. Lingemann[2], A. Nehrkorn, A. Nowack, I.M. Nugent, C. Pistone, O. Pooth, A. Stahl

Deutsches Elektronen-Synchrotron, Hamburg, Germany

M. Aldaya Martin, I. Asin, N. Bartosik, O. Behnke, U. Behrens, A.J. Bell, K. Borras, A. Burgmeier, A. Cakir, L. Calligaris, A. Campbell, S. Choudhury, F. Costanza, C. Diez Pardos, G. Dolinska, S. Dooling, T. Dorland, G. Eckerlin, D. Eckstein, T. Eichhorn, G. Flucke, E. Gallo, J. Garay Garcia, A. Geiser, A. Gizhko, P. Gunnellini, J. Hauk, M. Hempel[15], H. Jung, A. Kalogeropoulos, O. Karacheban[15], M. Kasemann, P. Katsas, J. Kieseler, C. Kleinwort, I. Korol, W. Lange, J. Leonard, K. Lipka, A. Lobanov, W. Lohmann[15], R. Mankel, I. Marfin[15], I.-A. Melzer-Pellmann, A.B. Meyer, G. Mittag, J. Mnich, A. Mussgiller, S. Naumann-Emme, A. Nayak, E. Ntomari, H. Perrey, D. Pitzl, R. Placakyte, A. Raspereza, B. Roland, M.Ö. Sahin, P. Saxena, T. Schoerner-Sadenius, M. Schröder, C. Seitz, S. Spannagel, K.D. Trippkewitz, R. Walsh, C. Wissing

University of Hamburg, Hamburg, Germany

V. Blobel, M. Centis Vignali, A.R. Draeger, J. Erfle, E. Garutti, K. Goebel, D. Gonzalez, M. Görner, J. Haller, M. Hoffmann, R.S. Höing, A. Junkes, R. Klanner, R. Kogler, T. Lapsien, T. Lenz, I. Marchesini, D. Marconi, M. Meyer, D. Nowatschin, J. Ott, F. Pantaleo[2], T. Peiffer, A. Perieanu, N. Pietsch, J. Poehlsen, D. Rathjens, C. Sander, H. Schettler, P. Schleper, E. Schlieckau, A. Schmidt, J. Schwandt, M. Seidel, V. Sola, H. Stadie, G. Steinbrück, H. Tholen, D. Troendle, E. Usai, L. Vanelderen, A. Vanhoefer, B. Vormwald

Institut für Experimentelle Kernphysik, Karlsruhe, Germany

M. Akbiyik, C. Barth, C. Baus, J. Berger, C. Böser, E. Butz, T. Chwalek, F. Colombo, W. De Boer, A. Descroix, A. Dierlamm, S. Fink, F. Frensch, M. Giffels, A. Gilbert,

F. Hartmann[2], S.M. Heindl, U. Husemann, I. Katkov[6], A. Kornmayer[2], P. Lobelle Pardo, B. Maier, H. Mildner, M.U. Mozer, T. Müller, Th. Müller, M. Plagge, G. Quast, K. Rabbertz, S. Röcker, F. Roscher, H.J. Simonis, F.M. Stober, R. Ulrich, J. Wagner-Kuhr, S. Wayand, M. Weber, T. Weiler, C. Wöhrmann, R. Wolf

Institute of Nuclear and Particle Physics (INPP), NCSR Demokritos, Aghia Paraskevi, Greece
G. Anagnostou, G. Daskalakis, T. Geralis, V.A. Giakoumopoulou, A. Kyriakis, D. Loukas, A. Psallidas, I. Topsis-Giotis

University of Athens, Athens, Greece
A. Agapitos, S. Kesisoglou, A. Panagiotou, N. Saoulidou, E. Tziaferi

University of Ioánnina, Ioánnina, Greece
I. Evangelou, G. Flouris, C. Foudas, P. Kokkas, N. Loukas, N. Manthos, I. Papadopoulos, E. Paradas, J. Strologas

Wigner Research Centre for Physics, Budapest, Hungary
G. Bencze, C. Hajdu, A. Hazi, P. Hidas, D. Horvath[16], F. Sikler, V. Veszpremi, G. Vesztergombi[17], A.J. Zsigmond

Institute of Nuclear Research ATOMKI, Debrecen, Hungary
N. Beni, S. Czellar, J. Karancsi[18], J. Molnar, Z. Szillasi

University of Debrecen, Debrecen, Hungary
M. Bartók[19], A. Makovec, P. Raics, Z.L. Trocsanyi, B. Ujvari

National Institute of Science Education and Research, Bhubaneswar, India
P. Mal, K. Mandal, N. Sahoo, S.K. Swain

Panjab University, Chandigarh, India
S. Bansal, S.B. Beri, V. Bhatnagar, R. Chawla, R. Gupta, U.Bhawandeep, A.K. Kalsi, A. Kaur, M. Kaur, R. Kumar, A. Mehta, M. Mittal, J.B. Singh, G. Walia

University of Delhi, Delhi, India
Ashok Kumar, A. Bhardwaj, B.C. Choudhary, R.B. Garg, A. Kumar, S. Malhotra, M. Naimuddin, N. Nishu, K. Ranjan, R. Sharma, V. Sharma

Saha Institute of Nuclear Physics, Kolkata, India
S. Banerjee, S. Bhattacharya, K. Chatterjee, S. Dey, S. Dutta, Sa. Jain, N. Majumdar, A. Modak, K. Mondal, S. Mukherjee, S. Mukhopadhyay, A. Roy, D. Roy, S. Roy Chowdhury, S. Sarkar, M. Sharan

Bhabha Atomic Research Centre, Mumbai, India
A. Abdulsalam, R. Chudasama, D. Dutta, V. Jha, V. Kumar, A.K. Mohanty[2], L.M. Pant, P. Shukla, A. Topkar

Tata Institute of Fundamental Research, Mumbai, India
T. Aziz, S. Banerjee, S. Bhowmik[20], R.M. Chatterjee, R.K. Dewanjee, S. Dugad, S. Ganguly, S. Ghosh, M. Guchait, A. Gurtu[21], G. Kole, S. Kumar, B. Mahakud, M. Maity[20],

G. Majumder, K. Mazumdar, S. Mitra, G.B. Mohanty, B. Parida, T. Sarkar[20], K. Sudhakar, N. Sur, B. Sutar, N. Wickramage[22]

Indian Institute of Science Education and Research (IISER), Pune, India
S. Chauhan, S. Dube, S. Sharma

Institute for Research in Fundamental Sciences (IPM), Tehran, Iran
H. Bakhshiansohi, H. Behnamian, S.M. Etesami[23], A. Fahim[24], R. Goldouzian, M. Khakzad, M. Mohammadi Najafabadi, M. Naseri, S. Paktinat Mehdiabadi, F. Rezaei Hosseinabadi, B. Safarzadeh[25], M. Zeinali

University College Dublin, Dublin, Ireland
M. Felcini, M. Grunewald

INFN Sezione di Bari [a], Università di Bari [b], Politecnico di Bari [c], Bari, Italy
M. Abbrescia[a,b], C. Calabria[a,b], C. Caputo[a,b], S.S. Chhibra[a,b], A. Colaleo[a], D. Creanza[a,c], L. Cristella[a,b], N. De Filippis[a,c], M. De Palma[a,b], L. Fiore[a], G. Iaselli[a,c], G. Maggi[a,c], M. Maggi[a], G. Miniello[a,b], S. My[a,c], S. Nuzzo[a,b], A. Pompili[a,b], G. Pugliese[a,c], R. Radogna[a,b], A. Ranieri[a], G. Selvaggi[a,b], L. Silvestris[a,2], R. Venditti[a,b], P. Verwilligen[a]

INFN Sezione di Bologna [a], Università di Bologna [b], Bologna, Italy
G. Abbiendi[a], C. Battilana[2], A.C. Benvenuti[a], D. Bonacorsi[a,b], S. Braibant-Giacomelli[a,b], L. Brigliadori[a,b], R. Campanini[a,b], P. Capiluppi[a,b], A. Castro[a,b], F.R. Cavallo[a], G. Codispoti[a,b], M. Cuffiani[a,b], G.M. Dallavalle[a], F. Fabbri[a], A. Fanfani[a,b], D. Fasanella[a,b], P. Giacomelli[a], C. Grandi[a], L. Guiducci[a,b], S. Marcellini[a], G. Masetti[a], A. Montanari[a], F.L. Navarria[a,b], A. Perrotta[a], A.M. Rossi[a,b], T. Rovelli[a,b], G.P. Siroli[a,b], N. Tosi[a,b], R. Travaglini[a,b]

INFN Sezione di Catania [a], Università di Catania [b], Catania, Italy
G. Cappello[a], M. Chiorboli[a,b], S. Costa[a,b], F. Giordano[a], R. Potenza[a,b], A. Tricomi[a,b], C. Tuve[a,b]

INFN Sezione di Firenze [a], Università di Firenze [b], Firenze, Italy
G. Barbagli[a], V. Ciulli[a,b], C. Civinini[a], R. D'Alessandro[a,b], E. Focardi[a,b], S. Gonzi[a,b], V. Gori[a,b], P. Lenzi[a,b], M. Meschini[a], S. Paoletti[a], G. Sguazzoni[a], A. Tropiano[a,b], L. Viliani[a,b]

INFN Laboratori Nazionali di Frascati, Frascati, Italy
L. Benussi, S. Bianco, F. Fabbri, D. Piccolo, F. Primavera

INFN Sezione di Genova [a], Università di Genova [b], Genova, Italy
V. Calvelli[a,b], F. Ferro[a], M. Lo Vetere[a,b], M.R. Monge[a,b], E. Robutti[a], S. Tosi[a,b]

INFN Sezione di Milano-Bicocca [a], Università di Milano-Bicocca [b], Milano, Italy
L. Brianza, M.E. Dinardo[a,b], S. Fiorendi[a,b], S. Gennai[a], R. Gerosa[a,b], A. Ghezzi[a,b], P. Govoni[a,b], S. Malvezzi[a], R.A. Manzoni[a,b], B. Marzocchi[a,b,2], D. Menasce[a], L. Moroni[a], M. Paganoni[a,b], D. Pedrini[a], S. Ragazzi[a,b], N. Redaelli[a], T. Tabarelli de Fatis[a,b]

INFN Sezione di Napoli [a], **Università di Napoli 'Federico II'** [b], **Napoli, Italy,**
Università della Basilicata [c], **Potenza, Italy, Università G. Marconi** [d], **Roma,**
Italy

S. Buontempo[a], N. Cavallo[a,c], S. Di Guida[a,d,2], M. Esposito[a,b], F. Fabozzi[a,c],
A.O.M. Iorio[a,b], G. Lanza[a], L. Lista[a], S. Meola[a,d,2], M. Merola[a], P. Paolucci[a,2],
C. Sciacca[a,b], F. Thyssen

INFN Sezione di Padova [a], **Università di Padova** [b], **Padova, Italy, Università di**
Trento [c], **Trento, Italy**

P. Azzi[a,2], N. Bacchetta[a], L. Benato[a,b], D. Bisello[a,b], A. Boletti[a,b], A. Branca[a,b],
R. Carlin[a,b], P. Checchia[a], M. Dall'Osso[a,b,2], T. Dorigo[a], F. Gasparini[a,b], U. Gasparini[a,b],
A. Gozzelino[a], K. Kanishchev[a,c], S. Lacaprara[a], M. Margoni[a,b], A.T. Meneguzzo[a,b],
M. Passaseo[a], J. Pazzini[a,b], M. Pegoraro[a], N. Pozzobon[a,b], P. Ronchese[a,b], F. Simonetto[a,b],
E. Torassa[a], M. Tosi[a,b], M. Zanetti, P. Zotto[a,b], A. Zucchetta[a,b,2], G. Zumerle[a,b]

INFN Sezione di Pavia [a], **Università di Pavia** [b], **Pavia, Italy**

A. Braghieri[a], A. Magnani[a], P. Montagna[a,b], S.P. Ratti[a,b], V. Re[a], C. Riccardi[a,b],
P. Salvini[a], I. Vai[a], P. Vitulo[a,b]

INFN Sezione di Perugia [a], **Università di Perugia** [b], **Perugia, Italy**

L. Alunni Solestizi[a,b], M. Biasini[a,b], G.M. Bilei[a], D. Ciangottini[a,b,2], L. Fanò[a,b],
P. Lariccia[a,b], G. Mantovani[a,b], M. Menichelli[a], A. Saha[a], A. Santocchia[a,b], A. Spiezia[a,b]

INFN Sezione di Pisa [a], **Università di Pisa** [b], **Scuola Normale Superiore di**
Pisa [c], **Pisa, Italy**

K. Androsov[a,26], P. Azzurri[a], G. Bagliesi[a], J. Bernardini[a], T. Boccali[a], G. Broccolo[a,c],
R. Castaldi[a], M.A. Ciocci[a,26], R. Dell'Orso[a], S. Donato[a,c,2], G. Fedi, L. Foà[a,c†],
A. Giassi[a], M.T. Grippo[a,26], F. Ligabue[a,c], T. Lomtadze[a], L. Martini[a,b], A. Messineo[a,b],
F. Palla[a], A. Rizzi[a,b], A. Savoy-Navarro[a,27], A.T. Serban[a], P. Spagnolo[a], P. Squillacioti[a,26],
R. Tenchini[a], G. Tonelli[a,b], A. Venturi[a], P.G. Verdini[a]

INFN Sezione di Roma [a], **Università di Roma** [b], **Roma, Italy**

L. Barone[a,b], F. Cavallari[a], G. D'imperio[a,b,2], D. Del Re[a,b], M. Diemoz[a], S. Gelli[a,b],
C. Jorda[a], E. Longo[a,b], F. Margaroli[a,b], P. Meridiani[a], F. Micheli[a,b], G. Organtini[a,b],
R. Paramatti[a], F. Preiato[a,b], S. Rahatlou[a,b], C. Rovelli[a], F. Santanastasio[a,b],
P. Traczyk[a,b,2]

INFN Sezione di Torino [a], **Università di Torino** [b], **Torino, Italy, Università del**
Piemonte Orientale [c], **Novara, Italy**

N. Amapane[a,b], R. Arcidiacono[a,c,2], S. Argiro[a,b], M. Arneodo[a,c], R. Bellan[a,b], C. Biino[a],
N. Cartiglia[a], M. Costa[a,b], R. Covarelli[a,b], D. Dattola[a], A. Degano[a,b], N. Demaria[a],
L. Finco[a,b,2], B. Kiani[a,b], C. Mariotti[a], S. Maselli[a], E. Migliore[a,b], V. Monaco[a,b],
E. Monteil[a,b], M. Musich[a], M.M. Obertino[a,b], L. Pacher[a,b], N. Pastrone[a], M. Pelliccioni[a],
G.L. Pinna Angioni[a,b], F. Ravera[a,b], A. Romero[a,b], M. Ruspa[a,c], R. Sacchi[a,b], A. Solano[a,b],
A. Staiano[a]

INFN Sezione di Trieste ^{a}, Università di Trieste ^{b}, Trieste, Italy

S. Belforte[a], V. Candelise[a,b,2], M. Casarsa[a], F. Cossutti[a], G. Della Ricca[a,b], B. Gobbo[a], C. La Licata[a,b], M. Marone[a,b], A. Schizzi[a,b], T. Umer[a,b], A. Zanetti[a]

Kangwon National University, Chunchon, Korea

A. Kropivnitskaya, S.K. Nam

Kyungpook National University, Daegu, Korea

D.H. Kim, G.N. Kim, M.S. Kim, D.J. Kong, S. Lee, Y.D. Oh, A. Sakharov, D.C. Son

Chonbuk National University, Jeonju, Korea

J.A. Brochero Cifuentes, H. Kim, T.J. Kim, M.S. Ryu

Chonnam National University, Institute for Universe and Elementary Particles, Kwangju, Korea

S. Song

Korea University, Seoul, Korea

S. Choi, Y. Go, D. Gyun, B. Hong, M. Jo, H. Kim, Y. Kim, B. Lee, K. Lee, K.S. Lee, S. Lee, S.K. Park, Y. Roh

Seoul National University, Seoul, Korea

H.D. Yoo

University of Seoul, Seoul, Korea

M. Choi, H. Kim, J.H. Kim, J.S.H. Lee, I.C. Park, G. Ryu

Sungkyunkwan University, Suwon, Korea

Y. Choi, Y.K. Choi, J. Goh, D. Kim, E. Kwon, J. Lee, I. Yu

Vilnius University, Vilnius, Lithuania

A. Juodagalvis, J. Vaitkus

National Centre for Particle Physics, Universiti Malaya, Kuala Lumpur, Malaysia

I. Ahmed, Z.A. Ibrahim, J.R. Komaragiri, M.A.B. Md Ali[28], F. Mohamad Idris[29], W.A.T. Wan Abdullah, M.N. Yusli

Centro de Investigacion y de Estudios Avanzados del IPN, Mexico City, Mexico

E. Casimiro Linares, H. Castilla-Valdez, E. De La Cruz-Burelo, I. Heredia-de La Cruz[30], A. Hernandez-Almada, R. Lopez-Fernandez, A. Sanchez-Hernandez

Universidad Iberoamericana, Mexico City, Mexico

S. Carrillo Moreno, F. Vazquez Valencia

Benemerita Universidad Autonoma de Puebla, Puebla, Mexico

I. Pedraza, H.A. Salazar Ibarguen

Universidad Autónoma de San Luis Potosí, San Luis Potosí, Mexico

A. Morelos Pineda

University of Auckland, Auckland, New Zealand

D. Krofcheck

University of Canterbury, Christchurch, New Zealand

P.H. Butler, S. Reucroft

National Centre for Physics, Quaid-I-Azam University, Islamabad, Pakistan

A. Ahmad, M. Ahmad, Q. Hassan, H.R. Hoorani, W.A. Khan, T. Khurshid, M. Shoaib

National Centre for Nuclear Research, Swierk, Poland

H. Bialkowska, M. Bluj, B. Boimska, T. Frueboes, M. Górski, M. Kazana, K. Nawrocki, K. Romanowska-Rybinska, M. Szleper, P. Zalewski

Institute of Experimental Physics, Faculty of Physics, University of Warsaw, Warsaw, Poland

G. Brona, K. Bunkowski, K. Doroba, A. Kalinowski, M. Konecki, J. Krolikowski, M. Misiura, M. Olszewski, M. Walczak

Laboratório de Instrumentação e Física Experimental de Partículas, Lisboa, Portugal

P. Bargassa, C. Beirão Da Cruz E Silva, A. Di Francesco, P. Faccioli, P.G. Ferreira Parracho, M. Gallinaro, N. Leonardo, L. Lloret Iglesias, F. Nguyen, J. Rodrigues Antunes, J. Seixas, O. Toldaiev, D. Vadruccio, J. Varela, P. Vischia

Joint Institute for Nuclear Research, Dubna, Russia

S. Afanasiev, P. Bunin, M. Gavrilenko, I. Golutvin, I. Gorbunov, A. Kamenev, V. Karjavin, V. Konoplyanikov, A. Lanev, A. Malakhov, V. Matveev[31], P. Moisenz, V. Palichik, V. Perelygin, S. Shmatov, S. Shulha, N. Skatchkov, V. Smirnov, A. Zarubin

Petersburg Nuclear Physics Institute, Gatchina (St. Petersburg), Russia

V. Golovtsov, Y. Ivanov, V. Kim[32], E. Kuznetsova, P. Levchenko, V. Murzin, V. Oreshkin, I. Smirnov, V. Sulimov, L. Uvarov, S. Vavilov, A. Vorobyev

Institute for Nuclear Research, Moscow, Russia

Yu. Andreev, A. Dermenev, S. Gninenko, N. Golubev, A. Karneyeu, M. Kirsanov, N. Krasnikov, A. Pashenkov, D. Tlisov, A. Toropin

Institute for Theoretical and Experimental Physics, Moscow, Russia

V. Epshteyn, V. Gavrilov, N. Lychkovskaya, V. Popov, I. Pozdnyakov, G. Safronov, A. Spiridonov, E. Vlasov, A. Zhokin

National Research Nuclear University 'Moscow Engineering Physics Institute' (MEPhI), Moscow, Russia

A. Bylinkin

P.N. Lebedev Physical Institute, Moscow, Russia

V. Andreev, M. Azarkin[33], I. Dremin[33], M. Kirakosyan, A. Leonidov[33], G. Mesyats, S.V. Rusakov, A. Vinogradov

Skobeltsyn Institute of Nuclear Physics, Lomonosov Moscow State University, Moscow, Russia

A. Baskakov, A. Belyaev, E. Boos, M. Dubinin[34], L. Dudko, A. Ershov, A. Gribushin, V. Klyukhin, O. Kodolova, I. Lokhtin, I. Myagkov, S. Obraztsov, S. Petrushanko, V. Savrin, A. Snigirev

State Research Center of Russian Federation, Institute for High Energy Physics, Protvino, Russia

I. Azhgirey, I. Bayshev, S. Bitioukov, V. Kachanov, A. Kalinin, D. Konstantinov, V. Krychkine, V. Petrov, R. Ryutin, A. Sobol, L. Tourtchanovitch, S. Troshin, N. Tyurin, A. Uzunian, A. Volkov

University of Belgrade, Faculty of Physics and Vinca Institute of Nuclear Sciences, Belgrade, Serbia

P. Adzic[35], M. Ekmedzic, J. Milosevic, V. Rekovic

Centro de Investigaciones Energéticas Medioambientales y Tecnológicas (CIEMAT), Madrid, Spain

J. Alcaraz Maestre, E. Calvo, M. Cerrada, M. Chamizo Llatas, N. Colino, B. De La Cruz, A. Delgado Peris, D. Domínguez Vázquez, A. Escalante Del Valle, C. Fernandez Bedoya, J.P. Fernández Ramos, J. Flix, M.C. Fouz, P. Garcia-Abia, O. Gonzalez Lopez, S. Goy Lopez, J.M. Hernandez, M.I. Josa, E. Navarro De Martino, A. Pérez-Calero Yzquierdo, J. Puerta Pelayo, A. Quintario Olmeda, I. Redondo, L. Romero, M.S. Soares

Universidad Autónoma de Madrid, Madrid, Spain

C. Albajar, J.F. de Trocóniz, M. Missiroli, D. Moran

Universidad de Oviedo, Oviedo, Spain

H. Brun, J. Cuevas, J. Fernandez Menendez, S. Folgueras, I. Gonzalez Caballero, E. Palencia Cortezon, J.M. Vizan Garcia

Instituto de Física de Cantabria (IFCA), CSIC-Universidad de Cantabria, Santander, Spain

I.J. Cabrillo, A. Calderon, J.R. Castiñeiras De Saa, P. De Castro Manzano, J. Duarte Campderros, M. Fernandez, J. Garcia-Ferrero, G. Gomez, A. Graziano, A. Lopez Virto, J. Marco, R. Marco, C. Martinez Rivero, F. Matorras, F.J. Munoz Sanchez, J. Piedra Gomez, T. Rodrigo, A.Y. Rodríguez-Marrero, A. Ruiz-Jimeno, L. Scodellaro, I. Vila, R. Vilar Cortabitarte

CERN, European Organization for Nuclear Research, Geneva, Switzerland

D. Abbaneo, E. Auffray, G. Auzinger, M. Bachtis, P. Baillon, A.H. Ball, D. Barney, A. Benaglia, J. Bendavid, L. Benhabib, J.F. Benitez, G.M. Berruti, P. Bloch, A. Bocci, A. Bonato, C. Botta, H. Breuker, T. Camporesi, G. Cerminara, S. Colafranceschi[36], M. D'Alfonso, D. d'Enterria, A. Dabrowski, V. Daponte, A. David, M. De Gruttola, F. De Guio, A. De Roeck, S. De Visscher, E. Di Marco, M. Dobson, M. Dordevic, B. Dorney, T. du Pree, M. Dünser, N. Dupont, A. Elliott-Peisert, G. Franzoni, W. Funk, D. Gigi, K. Gill, D. Giordano, M. Girone, F. Glege, R. Guida, S. Gundacker, M. Guthoff, J. Hammer,

P. Harris, J. Hegeman, V. Innocente, P. Janot, H. Kirschenmann, M.J. Kortelainen, K. Kousouris, K. Krajczar, P. Lecoq, C. Lourenço, M.T. Lucchini, N. Magini, L. Malgeri, M. Mannelli, A. Martelli, L. Masetti, F. Meijers, S. Mersi, E. Meschi, F. Moortgat, S. Morovic, M. Mulders, M.V. Nemallapudi, H. Neugebauer, S. Orfanelli[37], L. Orsini, L. Pape, E. Perez, M. Peruzzi, A. Petrilli, G. Petrucciani, A. Pfeiffer, D. Piparo, A. Racz, G. Rolandi[38], M. Rovere, M. Ruan, H. Sakulin, C. Schäfer, C. Schwick, A. Sharma, P. Silva, M. Simon, P. Sphicas[39], D. Spiga, J. Steggemann, B. Stieger, M. Stoye, Y. Takahashi, D. Treille, A. Triossi, A. Tsirou, G.I. Veres[17], N. Wardle, H.K. Wöhri, A. Zagozdzinska[40], W.D. Zeuner

Paul Scherrer Institut, Villigen, Switzerland
W. Bertl, K. Deiters, W. Erdmann, R. Horisberger, Q. Ingram, H.C. Kaestli, D. Kotlinski, U. Langenegger, D. Renker, T. Rohe

Institute for Particle Physics, ETH Zurich, Zurich, Switzerland
F. Bachmair, L. Bäni, L. Bianchini, M.A. Buchmann, B. Casal, G. Dissertori, M. Dittmar, M. Donegà, P. Eller, C. Grab, C. Heidegger, D. Hits, J. Hoss, G. Kasieczka, W. Lustermann, B. Mangano, A.C. Marini, M. Marionneau, P. Martinez Ruiz del Arbol, M. Masciovecchio, D. Meister, P. Musella, F. Nessi-Tedaldi, F. Pandolfi, J. Pata, F. Pauss, L. Perrozzi, M. Quittnat, M. Rossini, A. Starodumov[41], M. Takahashi, V.R. Tavolaro, K. Theofilatos, R. Wallny

Universität Zürich, Zurich, Switzerland
T.K. Aarrestad, C. Amsler[42], L. Caminada, M.F. Canelli, V. Chiochia, A. De Cosa, C. Galloni, A. Hinzmann, T. Hreus, B. Kilminster, C. Lange, J. Ngadiuba, D. Pinna, P. Robmann, F.J. Ronga, D. Salerno, Y. Yang

National Central University, Chung-Li, Taiwan
M. Cardaci, K.H. Chen, T.H. Doan, Sh. Jain, R. Khurana, M. Konyushikhin, C.M. Kuo, W. Lin, Y.J. Lu, R. Volpe, S.S. Yu

National Taiwan University (NTU), Taipei, Taiwan
Arun Kumar, R. Bartek, P. Chang, Y.H. Chang, Y.W. Chang, Y. Chao, K.F. Chen, P.H. Chen, C. Dietz, F. Fiori, U. Grundler, W.-S. Hou, Y. Hsiung, Y.F. Liu, R.-S. Lu, M. Miñano Moya, E. Petrakou, J.F. Tsai, Y.M. Tzeng

Chulalongkorn University, Faculty of Science, Department of Physics, Bangkok, Thailand
B. Asavapibhop, K. Kovitanggoon, G. Singh, N. Srimanobhas, N. Suwonjandee

Cukurova University, Adana, Turkey
A. Adiguzel, S. Cerci[43], Z.S. Demiroglu, C. Dozen, I. Dumanoglu, S. Girgis, G. Gokbulut, Y. Guler, E. Gurpinar, I. Hos, E.E. Kangal[44], A. Kayis Topaksu, G. Onengut[45], K. Ozdemir[46], S. Ozturk[47], B. Tali[43], H. Topakli[47], M. Vergili, C. Zorbilmez

Middle East Technical University, Physics Department, Ankara, Turkey
I.V. Akin, B. Bilin, S. Bilmis, B. Isildak[48], G. Karapinar[49], U.E. Surat, M. Yalvac, M. Zeyrek

Bogazici University, Istanbul, Turkey

E.A. Albayrak[50], E. Gülmez, M. Kaya[51], O. Kaya[52], T. Yetkin[53]

Istanbul Technical University, Istanbul, Turkey

K. Cankocak, S. Sen[54], F.I. Vardarlı

Institute for Scintillation Materials of National Academy of Science of Ukraine, Kharkov, Ukraine

B. Grynyov

National Scientific Center, Kharkov Institute of Physics and Technology, Kharkov, Ukraine

L. Levchuk, P. Sorokin

University of Bristol, Bristol, United Kingdom

R. Aggleton, F. Ball, L. Beck, J.J. Brooke, E. Clement, D. Cussans, H. Flacher, J. Goldstein, M. Grimes, G.P. Heath, H.F. Heath, J. Jacob, L. Kreczko, C. Lucas, Z. Meng, D.M. Newbold[55], S. Paramesvaran, A. Poll, T. Sakuma, S. Seif El Nasr-storey, S. Senkin, D. Smith, V.J. Smith

Rutherford Appleton Laboratory, Didcot, United Kingdom

K.W. Bell, A. Belyaev[56], C. Brew, R.M. Brown, D.J.A. Cockerill, J.A. Coughlan, K. Harder, S. Harper, E. Olaiya, D. Petyt, C.H. Shepherd-Themistocleous, A. Thea, L. Thomas, I.R. Tomalin, T. Williams, W.J. Womersley, S.D. Worm

Imperial College, London, United Kingdom

M. Baber, R. Bainbridge, O. Buchmuller, A. Bundock, D. Burton, S. Casasso, M. Citron, D. Colling, L. Corpe, N. Cripps, P. Dauncey, G. Davies, A. De Wit, M. Della Negra, P. Dunne, A. Elwood, W. Ferguson, J. Fulcher, D. Futyan, G. Hall, G. Iles, M. Kenzie, R. Lane, R. Lucas[55], L. Lyons, A.-M. Magnan, S. Malik, J. Nash, A. Nikitenko[41], J. Pela, M. Pesaresi, K. Petridis, D.M. Raymond, A. Richards, A. Rose, C. Seez, A. Tapper, K. Uchida, M. Vazquez Acosta[57], T. Virdee, S.C. Zenz

Brunel University, Uxbridge, United Kingdom

J.E. Cole, P.R. Hobson, A. Khan, P. Kyberd, D. Leggat, D. Leslie, I.D. Reid, P. Symonds, L. Teodorescu, M. Turner

Baylor University, Waco, U.S.A.

A. Borzou, K. Call, J. Dittmann, K. Hatakeyama, A. Kasmi, H. Liu, N. Pastika

The University of Alabama, Tuscaloosa, U.S.A.

O. Charaf, S.I. Cooper, C. Henderson, P. Rumerio

Boston University, Boston, U.S.A.

A. Avetisyan, T. Bose, C. Fantasia, D. Gastler, P. Lawson, D. Rankin, C. Richardson, J. Rohlf, J. St. John, L. Sulak, D. Zou

Brown University, Providence, U.S.A.

J. Alimena, E. Berry, S. Bhattacharya, D. Cutts, N. Dhingra, A. Ferapontov, A. Garabedian, U. Heintz, E. Laird, G. Landsberg, Z. Mao, M. Narain, S. Piperov, S. Sagir, T. Sinthuprasith, R. Syarif

University of California, Davis, Davis, U.S.A.

R. Breedon, G. Breto, M. Calderon De La Barca Sanchez, S. Chauhan, M. Chertok, J. Conway, R. Conway, P.T. Cox, R. Erbacher, M. Gardner, W. Ko, R. Lander, M. Mulhearn, D. Pellett, J. Pilot, F. Ricci-Tam, S. Shalhout, J. Smith, M. Squires, D. Stolp, M. Tripathi, S. Wilbur, R. Yohay

University of California, Los Angeles, U.S.A.

R. Cousins, P. Everaerts, C. Farrell, J. Hauser, M. Ignatenko, D. Saltzberg, E. Takasugi, V. Valuev, M. Weber

University of California, Riverside, Riverside, U.S.A.

K. Burt, R. Clare, J. Ellison, J.W. Gary, G. Hanson, J. Heilman, M. Ivova PANEVA, P. Jandir, E. Kennedy, F. Lacroix, O.R. Long, A. Luthra, M. Malberti, M. Olmedo Negrete, A. Shrinivas, H. Wei, S. Wimpenny

University of California, San Diego, La Jolla, U.S.A.

J.G. Branson, G.B. Cerati, S. Cittolin, R.T. D'Agnolo, A. Holzner, R. Kelley, D. Klein, J. Letts, I. Macneill, D. Olivito, S. Padhi, M. Pieri, M. Sani, V. Sharma, S. Simon, M. Tadel, A. Vartak, S. Wasserbaech[58], C. Welke, F. Würthwein, A. Yagil, G. Zevi Della Porta

University of California, Santa Barbara, Santa Barbara, U.S.A.

D. Barge, J. Bradmiller-Feld, C. Campagnari, A. Dishaw, V. Dutta, K. Flowers, M. Franco Sevilla, P. Geffert, C. George, F. Golf, L. Gouskos, J. Gran, J. Incandela, C. Justus, N. Mccoll, S.D. Mullin, J. Richman, D. Stuart, I. Suarez, W. To, C. West, J. Yoo

California Institute of Technology, Pasadena, U.S.A.

D. Anderson, A. Apresyan, A. Bornheim, J. Bunn, Y. Chen, J. Duarte, A. Mott, H.B. Newman, C. Pena, M. Pierini, M. Spiropulu, J.R. Vlimant, S. Xie, R.Y. Zhu

Carnegie Mellon University, Pittsburgh, U.S.A.

V. Azzolini, A. Calamba, B. Carlson, T. Ferguson, M. Paulini, J. Russ, M. Sun, H. Vogel, I. Vorobiev

University of Colorado Boulder, Boulder, U.S.A.

J.P. Cumalat, W.T. Ford, A. Gaz, F. Jensen, A. Johnson, M. Krohn, T. Mulholland, U. Nauenberg, K. Stenson, S.R. Wagner

Cornell University, Ithaca, U.S.A.

J. Alexander, A. Chatterjee, J. Chaves, J. Chu, S. Dittmer, N. Eggert, N. Mirman, G. Nicolas Kaufman, J.R. Patterson, A. Rinkevicius, A. Ryd, L. Skinnari, L. Soffi, W. Sun, S.M. Tan, W.D. Teo, J. Thom, J. Thompson, J. Tucker, Y. Weng, P. Wittich

Fermi National Accelerator Laboratory, Batavia, U.S.A.

S. Abdullin, M. Albrow, J. Anderson, G. Apollinari, L.A.T. Bauerdick, A. Beretvas, J. Berryhill, P.C. Bhat, G. Bolla, K. Burkett, J.N. Butler, H.W.K. Cheung, F. Chlebana, S. Cihangir, V.D. Elvira, I. Fisk, J. Freeman, E. Gottschalk, L. Gray, D. Green, S. Grünendahl, O. Gutsche, J. Hanlon, D. Hare, R.M. Harris, J. Hirschauer, B. Hooberman, Z. Hu, S. Jindariani, M. Johnson, U. Joshi, A.W. Jung, B. Klima, B. Kreis, S. Kwan[†], S. Lammel, J. Linacre, D. Lincoln, R. Lipton, T. Liu, R. Lopes De Sá, J. Lykken, K. Maeshima, J.M. Marraffino, V.I. Martinez Outschoorn, S. Maruyama, D. Mason, P. McBride, P. Merkel, K. Mishra, S. Mrenna, S. Nahn, C. Newman-Holmes, V. O'Dell, K. Pedro, O. Prokofyev, G. Rakness, E. Sexton-Kennedy, A. Soha, W.J. Spalding, L. Spiegel, L. Taylor, S. Tkaczyk, N.V. Tran, L. Uplegger, E.W. Vaandering, C. Vernieri, M. Verzocchi, R. Vidal, H.A. Weber, A. Whitbeck, F. Yang, H. Yin

University of Florida, Gainesville, U.S.A.

D. Acosta, P. Avery, P. Bortignon, D. Bourilkov, A. Carnes, M. Carver, D. Curry, S. Das, G.P. Di Giovanni, R.D. Field, M. Fisher, I.K. Furic, J. Hugon, J. Konigsberg, A. Korytov, J.F. Low, P. Ma, K. Matchev, H. Mei, P. Milenovic[59], G. Mitselmakher, L. Muniz, D. Rank, R. Rossin, L. Shchutska, M. Snowball, D. Sperka, J. Wang, S. Wang, J. Yelton

Florida International University, Miami, U.S.A.

S. Hewamanage, S. Linn, P. Markowitz, G. Martinez, J.L. Rodriguez

Florida State University, Tallahassee, U.S.A.

A. Ackert, J.R. Adams, T. Adams, A. Askew, J. Bochenek, B. Diamond, J. Haas, S. Hagopian, V. Hagopian, K.F. Johnson, A. Khatiwada, H. Prosper, V. Veeraraghavan, M. Weinberg

Florida Institute of Technology, Melbourne, U.S.A.

V. Bhopatkar, M. Hohlmann, H. Kalakhety, D. Mareskas-palcek, D. Noonan, T. Roy, F. Yumiceva

University of Illinois at Chicago (UIC), Chicago, U.S.A.

M.R. Adams, L. Apanasevich, D. Berry, R.R. Betts, I. Bucinskaite, R. Cavanaugh, O. Evdokimov, L. Gauthier, C.E. Gerber, D.J. Hofman, P. Kurt, C. O'Brien, I.D. Sandoval Gonzalez, C. Silkworth, P. Turner, N. Varelas, Z. Wu, M. Zakaria

The University of Iowa, Iowa City, U.S.A.

B. Bilki[60], W. Clarida, K. Dilsiz, S. Durgut, R.P. Gandrajula, M. Haytmyradov, V. Khristenko, J.-P. Merlo, H. Mermerkaya[61], A. Mestvirishvili, A. Moeller, J. Nachtman, H. Ogul, Y. Onel, F. Ozok[50], A. Penzo, C. Snyder, P. Tan, E. Tiras, J. Wetzel, K. Yi

Johns Hopkins University, Baltimore, U.S.A.

I. Anderson, B.A. Barnett, B. Blumenfeld, D. Fehling, L. Feng, A.V. Gritsan, P. Maksimovic, C. Martin, M. Osherson, M. Swartz, M. Xiao, Y. Xin, C. You

The University of Kansas, Lawrence, U.S.A.

P. Baringer, A. Bean, G. Benelli, C. Bruner, J. Gray, R.P. Kenny III, D. Majumder, M. Malek, M. Murray, S. Sanders, R. Stringer, Q. Wang, J.S. Wood

Kansas State University, Manhattan, U.S.A.

I. Chakaberia, A. Ivanov, K. Kaadze, S. Khalil, M. Makouski, Y. Maravin, A. Mohammadi, L.K. Saini, N. Skhirtladze, I. Svintradze, S. Toda

Lawrence Livermore National Laboratory, Livermore, U.S.A.

D. Lange, F. Rebassoo, D. Wright

University of Maryland, College Park, U.S.A.

C. Anelli, A. Baden, O. Baron, A. Belloni, B. Calvert, S.C. Eno, C. Ferraioli, J.A. Gomez, N.J. Hadley, S. Jabeen, R.G. Kellogg, T. Kolberg, J. Kunkle, Y. Lu, A.C. Mignerey, Y.H. Shin, A. Skuja, M.B. Tonjes, S.C. Tonwar

Massachusetts Institute of Technology, Cambridge, U.S.A.

A. Apyan, R. Barbieri, A. Baty, K. Bierwagen, S. Brandt, W. Busza, I.A. Cali, Z. Demiragli, L. Di Matteo, G. Gomez Ceballos, M. Goncharov, D. Gulhan, Y. Iiyama, G.M. Innocenti, M. Klute, D. Kovalskyi, Y.S. Lai, Y.-J. Lee, A. Levin, P.D. Luckey, C. Mcginn, C. Mironov, X. Niu, C. Paus, D. Ralph, C. Roland, G. Roland, J. Salfeld-Nebgen, G.S.F. Stephans, K. Sumorok, M. Varma, D. Velicanu, J. Veverka, J. Wang, T.W. Wang, B. Wyslouch, M. Yang, V. Zhukova

University of Minnesota, Minneapolis, U.S.A.

B. Dahmes, A. Finkel, A. Gude, P. Hansen, S. Kalafut, S.C. Kao, K. Klapoetke, Y. Kubota, Z. Lesko, J. Mans, S. Nourbakhsh, N. Ruckstuhl, R. Rusack, N. Tambe, J. Turkewitz

University of Mississippi, Oxford, U.S.A.

J.G. Acosta, S. Oliveros

University of Nebraska-Lincoln, Lincoln, U.S.A.

E. Avdeeva, K. Bloom, S. Bose, D.R. Claes, A. Dominguez, C. Fangmeier, R. Gonzalez Suarez, R. Kamalieddin, J. Keller, D. Knowlton, I. Kravchenko, J. Lazo-Flores, F. Meier, J. Monroy, F. Ratnikov, J.E. Siado, G.R. Snow

State University of New York at Buffalo, Buffalo, U.S.A.

M. Alyari, J. Dolen, J. George, A. Godshalk, I. Iashvili, J. Kaisen, A. Kharchilava, A. Kumar, S. Rappoccio

Northeastern University, Boston, U.S.A.

G. Alverson, E. Barberis, D. Baumgartel, M. Chasco, A. Hortiangtham, B. Knapp, A. Massironi, D.M. Morse, D. Nash, T. Orimoto, R. Teixeira De Lima, D. Trocino, R.-J. Wang, D. Wood, J. Zhang

Northwestern University, Evanston, U.S.A.

K.A. Hahn, A. Kubik, N. Mucia, N. Odell, B. Pollack, A. Pozdnyakov, M. Schmitt, S. Stoynev, K. Sung, M. Trovato, M. Velasco

University of Notre Dame, Notre Dame, U.S.A.

A. Brinkerhoff, N. Dev, M. Hildreth, C. Jessop, D.J. Karmgard, N. Kellams, K. Lannon, S. Lynch, N. Marinelli, F. Meng, C. Mueller, Y. Musienko[31], T. Pearson, M. Planer, A. Reinsvold, R. Ruchti, G. Smith, S. Taroni, N. Valls, M. Wayne, M. Wolf, A. Woodard

The Ohio State University, Columbus, U.S.A.

L. Antonelli, J. Brinson, B. Bylsma, L.S. Durkin, S. Flowers, A. Hart, C. Hill, R. Hughes, K. Kotov, T.Y. Ling, B. Liu, W. Luo, D. Puigh, M. Rodenburg, B.L. Winer, H.W. Wulsin

Princeton University, Princeton, U.S.A.

O. Driga, P. Elmer, J. Hardenbrook, P. Hebda, S.A. Koay, P. Lujan, D. Marlow, T. Medvedeva, M. Mooney, J. Olsen, C. Palmer, P. Piroué, X. Quan, H. Saka, D. Stickland, C. Tully, J.S. Werner, A. Zuranski

University of Puerto Rico, Mayaguez, U.S.A.

S. Malik

Purdue University, West Lafayette, U.S.A.

V.E. Barnes, D. Benedetti, D. Bortoletto, L. Gutay, M.K. Jha, M. Jones, K. Jung, M. Kress, D.H. Miller, N. Neumeister, B.C. Radburn-Smith, X. Shi, I. Shipsey, D. Silvers, J. Sun, A. Svyatkovskiy, F. Wang, W. Xie, L. Xu, J. Zablocki

Purdue University Calumet, Hammond, U.S.A.

N. Parashar, J. Stupak

Rice University, Houston, U.S.A.

A. Adair, B. Akgun, Z. Chen, K.M. Ecklund, F.J.M. Geurts, M. Guilbaud, W. Li, B. Michlin, M. Northup, B.P. Padley, R. Redjimi, J. Roberts, J. Rorie, Z. Tu, J. Zabel

University of Rochester, Rochester, U.S.A.

B. Betchart, A. Bodek, P. de Barbaro, R. Demina, Y. Eshaq, T. Ferbel, M. Galanti, A. Garcia-Bellido, P. Goldenzweig, J. Han, A. Harel, O. Hindrichs, A. Khukhunaishvili, G. Petrillo, M. Verzetti

The Rockefeller University, New York, U.S.A.

L. Demortier

Rutgers, The State University of New Jersey, Piscataway, U.S.A.

S. Arora, A. Barker, J.P. Chou, C. Contreras-Campana, E. Contreras-Campana, D. Duggan, D. Ferencek, Y. Gershtein, R. Gray, E. Halkiadakis, D. Hidas, E. Hughes, S. Kaplan, R. Kunnawalkam Elayavalli, A. Lath, K. Nash, S. Panwalkar, M. Park, S. Salur, S. Schnetzer, D. Sheffield, S. Somalwar, R. Stone, S. Thomas, P. Thomassen, M. Walker

University of Tennessee, Knoxville, U.S.A.

M. Foerster, G. Riley, K. Rose, S. Spanier, A. York

Texas A&M University, College Station, U.S.A.

O. Bouhali[62], A. Castaneda Hernandez, M. Dalchenko, M. De Mattia, A. Delgado, S. Dildick, R. Eusebi, W. Flanagan, J. Gilmore, T. Kamon[63], V. Krutelyov, R. Montalvo, R. Mueller, I. Osipenkov, Y. Pakhotin, R. Patel, A. Perloff, J. Roe, A. Rose, A. Safonov, A. Tatarinov, K.A. Ulmer[2]

Texas Tech University, Lubbock, U.S.A.

N. Akchurin, C. Cowden, J. Damgov, C. Dragoiu, P.R. Dudero, J. Faulkner, S. Kunori, K. Lamichhane, S.W. Lee, T. Libeiro, S. Undleeb, I. Volobouev

Vanderbilt University, Nashville, U.S.A.

E. Appelt, A.G. Delannoy, S. Greene, A. Gurrola, R. Janjam, W. Johns, C. Maguire, Y. Mao, A. Melo, H. Ni, P. Sheldon, B. Snook, S. Tuo, J. Velkovska, Q. Xu

University of Virginia, Charlottesville, U.S.A.

M.W. Arenton, S. Boutle, B. Cox, B. Francis, J. Goodell, R. Hirosky, A. Ledovskoy, H. Li, C. Lin, C. Neu, E. Wolfe, J. Wood, F. Xia

Wayne State University, Detroit, U.S.A.

C. Clarke, R. Harr, P.E. Karchin, C. Kottachchi Kankanamge Don, P. Lamichhane, J. Sturdy

University of Wisconsin, Madison, U.S.A.

D.A. Belknap, D. Carlsmith, M. Cepeda, A. Christian, S. Dasu, L. Dodd, S. Duric, E. Friis, B. Gomber, R. Hall-Wilton, M. Herndon, A. Hervé, P. Klabbers, A. Lanaro, A. Levine, K. Long, R. Loveless, A. Mohapatra, I. Ojalvo, T. Perry, G.A. Pierro, G. Polese, I. Ross, T. Ruggles, T. Sarangi, A. Savin, A. Sharma, N. Smith, W.H. Smith, D. Taylor, N. Woods

†: Deceased
1: Also at Vienna University of Technology, Vienna, Austria
2: Also at CERN, European Organization for Nuclear Research, Geneva, Switzerland
3: Also at State Key Laboratory of Nuclear Physics and Technology, Peking University, Beijing, China
4: Also at Institut Pluridisciplinaire Hubert Curien, Université de Strasbourg, Université de Haute Alsace Mulhouse, CNRS/IN2P3, Strasbourg, France
5: Also at National Institute of Chemical Physics and Biophysics, Tallinn, Estonia
6: Also at Skobeltsyn Institute of Nuclear Physics, Lomonosov Moscow State University, Moscow, Russia
7: Also at Universidade Estadual de Campinas, Campinas, Brazil
8: Also at Centre National de la Recherche Scientifique (CNRS) - IN2P3, Paris, France
9: Also at Joint Institute for Nuclear Research, Dubna, Russia
10: Also at Ain Shams University, Cairo, Egypt
11: Now at British University in Egypt, Cairo, Egypt
12: Also at Zewail City of Science and Technology, Zewail, Egypt
13: Also at Université de Haute Alsace, Mulhouse, France
14: Also at Tbilisi State University, Tbilisi, Georgia
15: Also at Brandenburg University of Technology, Cottbus, Germany
16: Also at Institute of Nuclear Research ATOMKI, Debrecen, Hungary
17: Also at Eötvös Loránd University, Budapest, Hungary
18: Also at University of Debrecen, Debrecen, Hungary
19: Also at Wigner Research Centre for Physics, Budapest, Hungary
20: Also at University of Visva-Bharati, Santiniketan, India
21: Now at King Abdulaziz University, Jeddah, Saudi Arabia

22: Also at University of Ruhuna, Matara, Sri Lanka
23: Also at Isfahan University of Technology, Isfahan, Iran
24: Also at University of Tehran, Department of Engineering Science, Tehran, Iran
25: Also at Plasma Physics Research Center, Science and Research Branch, Islamic Azad University, Tehran, Iran
26: Also at Università degli Studi di Siena, Siena, Italy
27: Also at Purdue University, West Lafayette, U.S.A.
28: Also at International Islamic University of Malaysia, Kuala Lumpur, Malaysia
29: Also at Malaysian Nuclear Agency, MOSTI, Kajang, Malaysia
30: Also at Consejo Nacional de Ciencia y Tecnología, Mexico city, Mexico
31: Also at Institute for Nuclear Research, Moscow, Russia
32: Also at St. Petersburg State Polytechnical University, St. Petersburg, Russia
33: Also at National Research Nuclear University 'Moscow Engineering Physics Institute' (MEPhI), Moscow, Russia
34: Also at California Institute of Technology, Pasadena, U.S.A.
35: Also at Faculty of Physics, University of Belgrade, Belgrade, Serbia
36: Also at Facoltà Ingegneria, Università di Roma, Roma, Italy
37: Also at National Technical University of Athens, Athens, Greece
38: Also at Scuola Normale e Sezione dell'INFN, Pisa, Italy
39: Also at University of Athens, Athens, Greece
40: Also at Warsaw University of Technology, Institute of Electronic Systems, Warsaw, Poland
41: Also at Institute for Theoretical and Experimental Physics, Moscow, Russia
42: Also at Albert Einstein Center for Fundamental Physics, Bern, Switzerland
43: Also at Adiyaman University, Adiyaman, Turkey
44: Also at Mersin University, Mersin, Turkey
45: Also at Cag University, Mersin, Turkey
46: Also at Piri Reis University, Istanbul, Turkey
47: Also at Gaziosmanpasa University, Tokat, Turkey
48: Also at Ozyegin University, Istanbul, Turkey
49: Also at Izmir Institute of Technology, Izmir, Turkey
50: Also at Mimar Sinan University, Istanbul, Istanbul, Turkey
51: Also at Marmara University, Istanbul, Turkey
52: Also at Kafkas University, Kars, Turkey
53: Also at Yildiz Technical University, Istanbul, Turkey
54: Also at Hacettepe University, Ankara, Turkey
55: Also at Rutherford Appleton Laboratory, Didcot, United Kingdom
56: Also at School of Physics and Astronomy, University of Southampton, Southampton, United Kingdom
57: Also at Instituto de Astrofísica de Canarias, La Laguna, Spain
58: Also at Utah Valley University, Orem, U.S.A.
59: Also at University of Belgrade, Faculty of Physics and Vinca Institute of Nuclear Sciences, Belgrade, Serbia
60: Also at Argonne National Laboratory, Argonne, U.S.A.
61: Also at Erzincan University, Erzincan, Turkey
62: Also at Texas A&M University at Qatar, Doha, Qatar
63: Also at Kyungpook National University, Daegu, Korea